ADDIS ABABA UNIVERSITY

ADDIS ABABA INSTITUTE OF TECHNOLOGY

SCHOOL OF MECHANICAL AND INDUSTRIAL ENGINEERING

Fatigue wear analysis and life prediction of rail under dry and lubricated wheel/rail contact conditions

A Thesis Submitted to the Graduate School of Addis Ababa University in Partial Fulfillment of the Requirements for the Degree of Masters of Science

In

Railway Engineering

(Rolling Stock)

By

Tsion Goa

Advisor

Mr. Habtamu Tkubet (Msc)

June 2017

ADDIS ABABA UNIVERSITY

ADDIS ABABA INSTITUTE OF TECHNOLOGY

SCHOOL OF MECHANICAL AND INDUSTRIAL ENGINEERING

Fatigue wear analysis and life prediction of rail under dry and lubricated wheel/rail contact conditions

By

Tsion Goa

Approved by Board of Examiners:

Mr. Habtamu Tkubet (MSc)	_____	_____
Advisor	Signature	Date
Mr. Araya Abera(Phd. Candidate)	_____	_____
Internal Examiner	Signature	Date
Dr.-Ing. Wondwossen Bogale	_____	_____
External Examiner	Signature	Date
Dr. Daniel Tilahun	_____	_____
Railway Center Head	Signature	Date

DECLARATION

I, the undersigned, declare that this thesis entitled "**Fatigue wear analysis and life prediction of rail under dry and lubricated wheel/rail contact conditions**" is my original work and has not been presented for any degree in any university and all the sources of materials used for the thesis have been duly acknowledged.

Tsion Goa _____ _____

Name Signature Date

ACKNOWLEDGEMENT

First and foremost thanks to Almighty GOD for his blessings throughout my research work.

I would like to present my special thanks to my advisor Mr. Habtamu Tkubet (MSc) for his valuable support and guide throughout this thesis work.

I am grateful to the Ethiopian Railway Corporation, which has given me this chance to study masters of degree at Addis Ababa Institute of technology. My deepest acknowledgement is extended to the staff of Ethiopian Railway Corporation for providing the necessary input information for this research.

Finally I would like to express my very profound gratitude to my family and friends for their patience, advice, moral support and motivation throughout this study. They kept me going, and this work would have not been possible without them.

ABSTRACT

The rail is subjected to high contact stress of alternating magnitude due to wheel-rail frictional rolling contact. Due to this the rail is prone to fatigue damage. This thesis paper addresses the fatigue problem by developing the contact between wheel and rail and predicting the fatigue life of the rail under dry and lubricated contact. Different values of friction coefficients are selected to model the dry (μ=0.6) and lubricated (μ=0.2 and μ=0.05) wheel/rail contact conditions in this study. The main objective of this is to study the effects of these varying friction coefficients on the fatigue life of the rail, so that better maintenance schedule can be implemented to increase the life of the rail. Analytical and numerical approaches are implemented in this thesis. The analytical approach investigates the Normal contact problem and tangential contact problem at the wheel/rail contact using the Hertz normal contact theory, Polach's tangential theories respectively. The numerical approach is based on the static structural analysis of the wheel/rail contact using ANSYS 15.0 commercial software. Three dimensional finite element method is utilized to investigate the effect of friction on the wheel/rail contact stress and the fatigue life of the rail. The fatigue life analysis is done using stress-life analyses approach. From the results found it can be seen that the fatigue life of the rail induced under dry wheel/rail contact conditions is minimum compared to the lubricated contact conditions. The fatigue life (in terms of cycles to failure) is 3689.4 cycles under dry contact, and 37834 cycles under water lubricated and 1.08e5 cycles under grease lubricated conditions. And the damage of the rail is higher under dry contact condition compared to lubricated contact conditions. This thesis is applicable for the Addis Ababa light rail operating system, in protecting the rail from fatigue failure. Managing the friction coefficient on the rail is recommended on the results.

Key words: Dry/Lubricated wheel/rail contact, Fatigue life, Finite element method, Rail

TABLE OF CONTENTS

LIST OF TABLES

LIST OF FIGURES

NOMENCLATURES

AA-LRT	Addis Ababa light transit system
COF	Coefficient of friction
FEM	Finite element method
3D	Three dimensional
a	Semi- major axis of contact patch
b	Semi- minor axis of contact patch
A & B	Geometric coefficient of Hertz contact theory
C_{ij}	Kalker's coefficient
E	Young's Modulus
E*	Equivalent Young's Modulus
ε	Gradient of tangential stress
F_N	Normal force
G	Modulus of rigidity
μ	Coefficient of friction
m, n	Constants in Hertz theory
P_o	Maximum contact pressure
Q	Traction force
υ	Poisson's ratio
V	Velocity
ω	Rotational velocity
ξ	Longitudinal creepage

CHAPTER ONE: INTRODUCTION

1.1. Background of the research

The rail way transport is one of the best and effective as well as environmental friendly land transport system. The performance of railway transport system is passing through a momentous improvement with, increasing speed, high axle load and rising traffic intensity.

Railway history in Ethiopia dates a while back, with the construction of a 784 Km railway in 1917 linking the capital Addis Ababa with the port of Djibouti [1]. But the operation was phased out (disrupted) due to major damages caused by out-dated and disrepair components as well as absence of maintenance and repair.

After being neglected for many years the railway service revived with a new, modern and larger network in 2010. This National railway Network of Ethiopia and the Addis Ababa light rail is aimed to link the capital Addis Ababa and various regions of the country and also too neighboring countries and ports, which is under the countries five-year transformation plan [2].

Some of these railway networks are under construction and some are under operation like the Addis Ababa light rail transit system which started operation in 2015. The introduction of this light rail system has made Ethiopia to be the first Sub-Saharan African country with this experience.

Unlike the old rail transport system to fully and effectively attend the benefits of this new railway system, effective management, and proper maintenance and damage prevention mechanism of wheel-rail contact should be implemented.

For effective and economical operation of a railway network, tribological issues must be highly paid attention, especially at the wheel-rail contact surface [3]. Tribology is the science and technology of friction, wear and lubrication of interacting surfaces in relative motion [4].

The wheel-rail interface is a crucial part in the successful operation of railways and key area of study. It is widely acknowledged that many of engineering problems within the railway industry arise at the interface between wheel and rail [4].

This study presents the fatigue life prediction of rail from a tribological point of view. The wheel-rail contact is an open system, so it is affected by contaminants, which can seriously affect the contact condition and the forces transmitted through the contact.

Wheel-rail contacts act as stress concentration areas, and are thus probable locations for mechanical failures. Stresses, contact pressures, elastic and plastic deformations caused by the wheel/rail contact are important parameters in terms of the service-life of the components and driving safety. Excessive stress at the wheel/rail contact leads to severe wear damage and surface damage [4]. The rail is subjected to high contact stress of alternating magnitude due to wheel-rail frictional rolling contact which can lead to fatigue damage of the rail.

Therefore better understanding and maintenance of the wheel-rail interface is necessary for improving reliability, capacity and safety of the railway system. The main tribological components reviewed in this study are lubricants, friction and fatigue wear. The wheel/rail contact condition is classified as dry and lubricated based on the third body materials present. These conditions can result in varying coefficient of friction which can further affect the fatigue life of the rail. The purpose of this thesis is to explore the effect of these dry and lubricated wheel/rail contact conditions on the effect of fatigue performance of the rail.

1.1.1. Dry and Lubricated Wheel/Rail Contact Conditions

As the wheel-rail contact is an open system, the contact is inevitably affected by contaminants. Contaminants refer to third body material present between wheel and rail [5]. These third body materials can be present due to naturally occurring conditions such as humidity, rain or leaves or products applied to the rail or wheel for a particular purpose such as oil (grease), friction modifiers and traction gels [5]. The wheel/rail contact can be classified as dry and lubricated contact condition based on these third body materials in this study.

In dry wheel/rail contact condition a third body layer exists which is thick layer of oxides [4] on the wheel-rail surfaces. Under lubricated condition the term "lubricants" (from a tribological perspective) refers to liquid contaminants present between wheel and rail. These contaminants can be "natural third body materials" present like water and "artificial third body materials" ones like grease.

Water can be present on the rail surface through heavy/light rain, drizzle, dew or misty conditions. Water is considered as a weak lubricant, which is enough to reduce friction but because of the small size it cannot form a protective film [6]. Grease is the main artificial rail contaminant (lubricant). Grease is applied by most railways on rail curves, to reduce friction and wear. Not enough is known about its behavior in a railway operating environment, but it can dramatically reduce the friction coefficient [6].

There are three lubrication regimes for liquid lubricants based on the Stribeck Curve [7]. The first one is Boundary lubrication, where constant contact occurs between two surfaces despite the presence of lubricant. The second one is mixed lubrication, where the two surfaces partially in contact and partially separated by lubricant. And the third regime is hydrodynamic lubrication, where the two surface separated by the lubricant film.

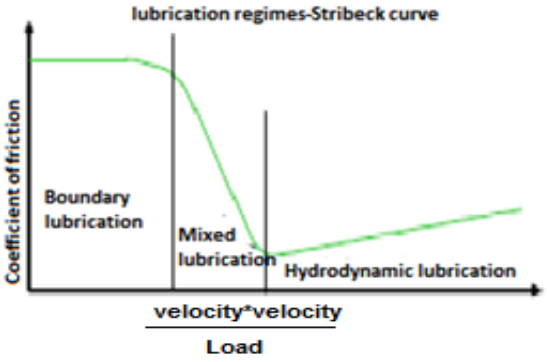

Figure 1.1-1: Lubrication regimes [7]

In the current AA-LRT operating system the above mention wheel/rail contact conditions exist. While rain is a naturally occurring lubricant which falls under boundary lubrication regime [7], grease is applied on the rail for the purpose of reducing friction, which falls under boundary to mixed lubrication regime [7]. The lubricants selected in this thesis are categorized under boundary lubricants, where constant contact occurs between the wheel and rail.

1.1.2. Friction at wheel/rail contact

The severity of the wheel-rail interface processes such as wear, Rolling contact fatigue (RCF) and noise are majorly controlled by frictional conditions [4]. The friction force is defined as the resistance encountered by one body moving over another body in both sliding and rolling bodies [4]. The friction between the wheels and rail plays a major role in the wheel/rail contact interface.

The wheel/rail contact is generally divided into two types of contacts, wheel tread-rail head contact along straight track and wheel flange-rail gauge contact along the curved rail. Ideal friction conditions in these wheel-rail contact regions are proposed as follows [8].

- Wheel tread-rail head contact: $0.25<\mu<0.4$
- Wheel flange-rail gauge contact: $\mu<0.1$

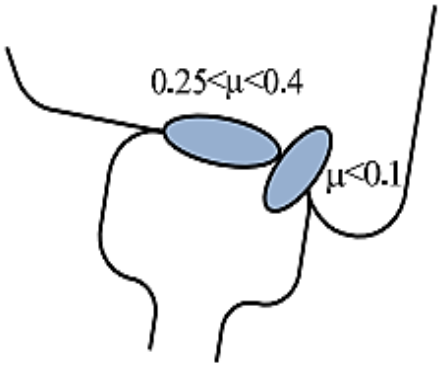

Figure 1.1-2: Ideal Friction coefficient at the wheel/rail contact [8]

To be able to find out the friction coefficient for two body surfaces in contact, a large number of variables need to be known, as friction is a system response and not decided by material parameters only. As a result of the difficulties of determining all parameters, it is therefore in many cases only possible to give rough estimation for the friction coefficient.

The wheel-rail contact is an open system, which makes it extremely difficult to transfer knowledge from other well-studied, but closed systems [6]. For example, the friction coefficient on the rail head is high on a sunny day but decreases on rainy day. Even on a sunny day, the friction coefficient can differ depending on the humidity and temperature. In addition, foreign substances, such as sand, dust, leaves, oil or grease can be present on the rail. All these factors will influence the friction coefficient, resulting in excessive or insufficient friction coefficient.

Numerous experiments have been conducted to study the friction of wheel/rail contact surfaces. The following figure shows the measured coefficient of friction at the managed wheel/rail interface, which vary widely from 0.05 to 0.7, under different conditions.

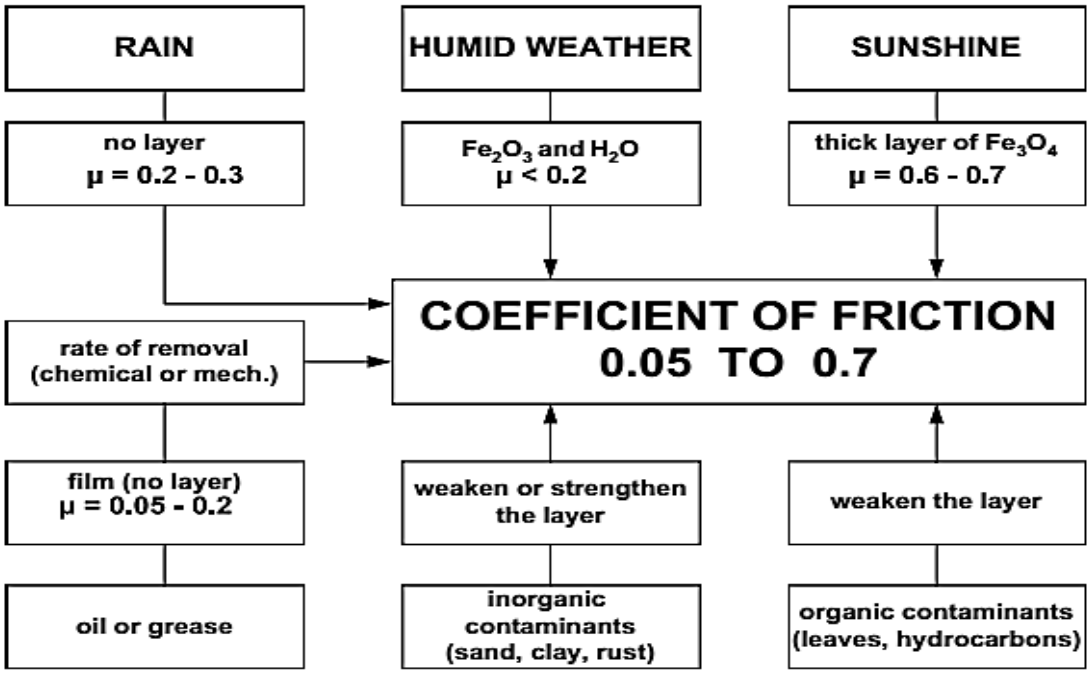

Figure 1.1-3: Friction Coefficient measured under different conditions [7]

Olofsson [4] compared the coefficient of friction measured on the track and in the laboratory. For non-lubricated tests (dry contact), the value was roughly the same and varied 0.5 and 0.6. For a full-scale lubricated rail (wet and oil) the coefficient of friction was lower and changed in the range of 0.2 to 0.4.

Another measurement conducted by Rovira [34] with twin disc experiment with real wheel-rail contact conditions (dry, wet, oil) to obtain the friction values under different contact pressures. The values of friction are listed below.

Pressure	Dry	Wet	Oil
1500	0.49	0.17	0.06
900	0.61	0.20	0.05

Table 1.1-1: Constant COF for 1500 MPa and 900 MPa contact pressure

So based on the above measurements made by different scholars, the following COF's are selected for this study. For dry contact condition a COF (μ=0.6) is selected, under water contact COF (μ=0.2) and grease lubricated (μ=0.05) are selected.

The effect of coefficient of friction between wheel and rail if not addressed well, it can lead to damage formation. In case too high, it can cause wear and surface fatigue damages to the wheel/rail system. And in case it is too low, it reduces the ability of the train to accelerate and brake properly [8].

The management of coefficient of friction is not addressed well, in AA-LRT operating system. This affects the smooth operating system of the railway. This paper mainly focuses on the effect of this un-managed coefficient of friction's under different wheel-rail contact conditions on the fatigue life of the rail.

Based on the wheel/rail contact conditions dry contact, water lubricated and grease lubricated conditions friction coefficients are selected from figure 3, for this study case.

1.1.3. Fatigue wear

Wear is the major cause of material wastage and loss of mechanical performance. Any reduction in wear can result in considerable savings [4]. Fatigue wear is one of the main types of wear. It is a term commonly used for surface damage caused by a repeated rolling contact. It is observed more frequently in the field of wheel/rail contact, as it is rolling /sliding system.

Contacts between asperities accompanied by very high local stresses are repeated a large number of times in the course of sliding or rolling with or without lubrication and wear particles are generated by fatigue propagated cracks, hence the term 'fatigue wear'[10]. Fatigue formation on rails due to repeated alternating tribological stress cycle is studied in this paper.

The term 'contact fatigue' is the technical term used in this study for this fatigue wear caused by a repeated rolling contact.

Fatigue is determined by the mechanism of the action of stress produced by rolling/sliding contact causing cracks to initiate and propagate, leading the surface to delaminate (mode of failure of splitting apart into layers).

High stress formed at the contact between wheel and rail lead to severe plastic deformation. When this accumulated high plastic deformation exceeds the critical shear stress, it causes crack initiation, crack growth and fracture. The cracks connect to each other, resulting in separation and delamination of the rail [10]. Mechanism of contact fatigue can be classified into two:

A) Mechanisms of fatigue wear under Rolling contact

During rolling the local contact stresses are very high concentrated over a small area and repetitive, and wear mechanisms are determined mostly by material characteristics and operating conditions illustrated schematically in figure below. The following figure shows fatigue crack formation under dry (un-lubricated) as well as lubricated rolling conditions.

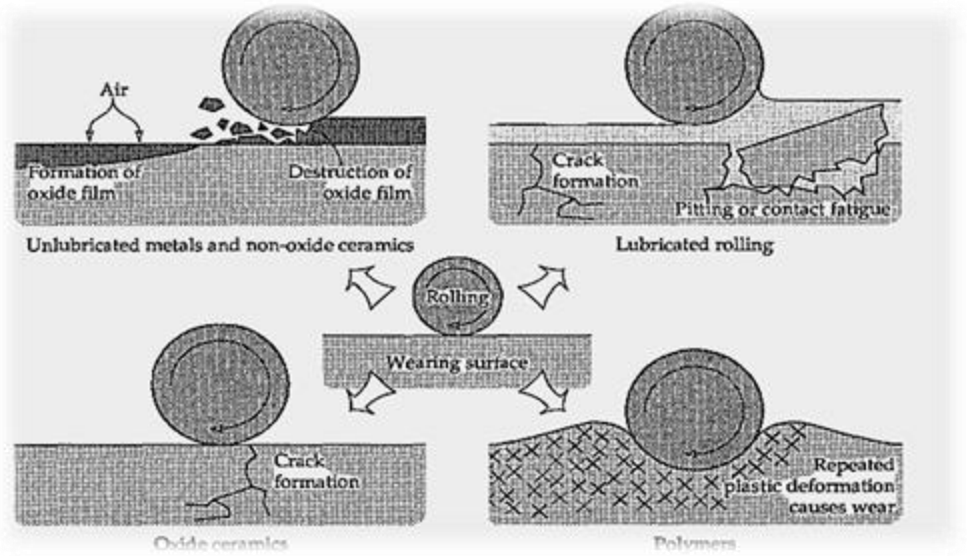

Figure 1.1-4: Mechanism of fatigue wear during rolling [10]

B) Mechanisms of fatigue wear under sliding contact

The Mechanism of surface crack initiated fatigue wear is illustrated schematically in the following figure. As it can be observed from the picture fatigue can be formed under adhesion or high friction.

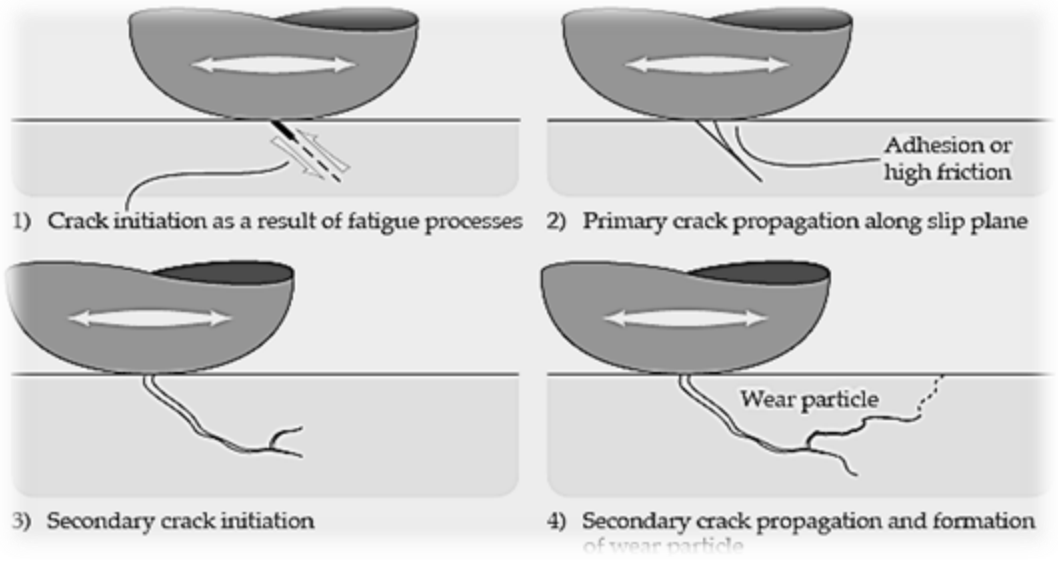

Figure 1.1-5: Mechanism of fatigue wear during sliding [10]

Since wheel/rail is a rolling/sliding contact fatigue can be damaged from fatigue failure. Fatigue failures of rails can be categorized into surface and subsurface failures. The cracks formed can be surface or sub-surface cracks, which results when the surface and subsurface cyclic shear stresses or strains in the material exceeds the fatigue limit for the material. Surface fatigue in rails can lead to head checking or squat formation, and subsurface fatigue can result in shelling or the formation of tache ovale [5].

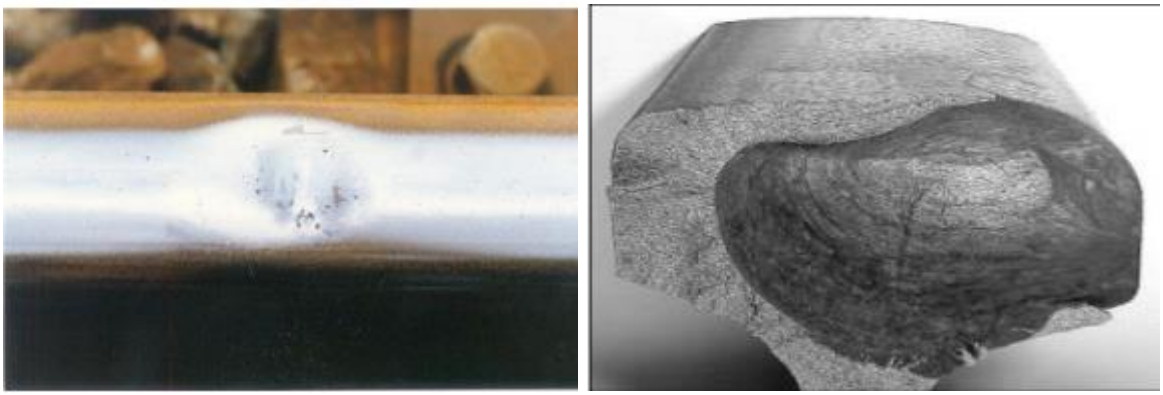

Figure 1.1-6: Surface fatigue: Rail squat (left), Sub-surface fatigue: Tache Ovale (right) [20]

If undetected early fatigue will cause derailment which in turn leads to loss of life and property, so the understanding of rail fatigue is important in reducing damages on the surface of rail. The Hatfield rail crash can be a good example. The Hatfield rail crash is a railway crash on October 17, 2000 in UK, it was caused by fatigue induced derailment, which incurred four deaths and 39 injured [7]. And also fatigue can increase the maintenance and replacement costs of the rail, if undetected early. Rail maintenance was estimated to have cost 300 million Euros within the European Union in 1995 [7], so gaining a good understanding of the contact and how it is affected by changing conditions is critical to designing methods to optimize its performance.

Generally based on the above given general background this study is performed to the study fatigue problem under dry and lubricated wheel/rail contact conditions by varying the coefficient of friction. And predict the life of the rail in AA-LRT.

1.2. Organization of the thesis

This thesis contains five chapters presenting the study. Chapter one is the introduction part, which outlines general information about the research conducted. Initially research background and organization of the thesis is discussed and presented. This is followed by the statement of problem and significance of the research. After that, the objective of this research is presented. Finally, the scope and limitation of this research are pointed out. Chapter two is the literature review part which comprehensively presents the background knowledge related to this research .The first part reviews wheel-rail contact theories. Then the overview of Finite element analysis on wheel-rail contact will be discussed. And then at last an overview of fatigue damage formation on the rail will be presented. Theoretical and numerical (Finite Element Method) Analysis is described in chapter three. First the Analytical analysis will be employed and then the Solid works will be used to model the wheel and rail profiles. After that Finite element method by using ANSYS will be utilized to investigate stress states and fatigue life of the rail. Chapter four describes the results and discussion of the study. The main findings of study are presented summarized in Chapter five along with recommendation and future works.

1.3. Statement of problem

Fatigue wear is a major problem at the wheel/rail contact that appears on rails due to high cyclic stress on the rail material. This fatigue failure can result in high maintenance cost, interruption in operating system, more over it can lead to accidents, if not predicted and prevented earlier. So this fatigue failure problem must be given high emphasis for smooth operating system of the AA-LRT.

Third body materials (contaminants) are present on the rail, and the friction of coefficient vary due to these contaminants. Based on these contaminants the wheel/rail contact is divided to dry and lubricated wheel/rail contact conditions. So this study focuses on the effect of these varying coefficients of friction under dry and lubricated contacts on the fatigue life of the rail. Generally this research tries to address the following questions.

- How do dry and lubricated wheel-rail contact conditions affect the wheel-rail interface?

- What will be the normal and tangential wheel/rail contact response under dry and lubricated conditions?
- What is the effect of varying friction coefficient on the contact stress distribution in wheel-rail contact?
- What is the fatigue life and damage of the rail under these varying friction coefficients due to dry and lubricated condition?

1.4. Significance of the research

Wheel/rail interface is main part where damages are caused in railway system. High stresses and forces are caused at this interface which can cause more frequent damage to the rail track, such as fatigue failure. Fatigue is a series problem, so this study helps to address fatigue damage caused at the rail track under dry and lubricated contact conditions, so that the following significance for the AA-LRT can be achieved:-

- A better planning of prevention and maintenance mechanisms will be implemented to maximize the service life of the rail at the AA-LRT operation system.
- Minimizes the maintenance and replacement cost of the rail from fatigue failure
- Smooth and safer railway operation system will be implemented

1.5. Objective

1.5.1. General Objective

The main objective of this research is to predict the fatigue life of the rail under dry and lubricated contact conditions on straight track by using three-dimensional finite element method. This is achieved by addressing the following specific objectives:-

1.5.2. Specific Objective

- Perform Analytical analysis of Normal and tangential contact problems at the wheel/rail contact using Hertz normal contact theory and Polach's tangential theory.
- Develop three dimensional modeling of wheel and rail based on the AA-LRT profiles

- Structural static analysis using ANSYS 15.0 Software
- Investigate the contact pressure and contact stress by using finite element analysis method on the wheel/rail contact under varying friction coefficients.
- Determine Fatigue life of the rail under dry and lubricated condition by using stress life method in ANSYS.

1.6. General Methodology

To fulfill the objectives of this study the methods used are:-

- Reviewing literatures related to this study done by different scholars
- Gathering wheel-rail geometrical data.
- CAD modeling:-SOLIDWORKS 2013 is used for modeling of three dimensional wheel/rail profiles
- Analysis:- ANSYS 15.0 software is used for static structural analysis and fatigue analysis

1.7. Scope and Limitation

1.7.1. Scope

Predicting fatigue life of the rail is the main scope of this study, taking into consideration dry and lubricated wheel-rail contact conditions. The analysis is carried with respect to AA-LRT wheel/rail profiles, speed and loading conditions. 3D finite element method is applied to evaluate the wheel-rail rolling contact stresses and fatigue life on a straight track. Different values of friction coefficients are chosen to model the dry and lubricated conditions.

1.7.2. Limitation

Due to the complexity of the modeling and time limitation factors, the following aspects are considered to be outside the scope of this research.

- Curved and transition track Scenario
- Canted rail and sub-components of the track(sleepers, rail pads and ballast)
- Prediction of Crack initiation and crack propagation at the rail
- Rail dynamic effects like vibration.

CHAPTER TWO: LITERATURE REVIEW

2.1. Introduction

In the literature, considerable researches are reviewed, which are performed in different areas related to this research. Some of the researches have direct relation to this study whereas others have indirect relations.

The literature review is organized as the following: Initially it will start with evolution of wheel-rail contact theories, and then next part contains a summery on wheel/rail contact conditions and FEM analysis done by different scholars, and at last the overview of fatigue damage formation.

2.2. Evolution of wheel-rail contact Theories

When studying wheel-rail contact conditions, it is worth mentioning some of the traditional theories which have led to this day transformation. The theories are divided into two [12], which are normal and tangential contact theories.

For normal wheel-rail contact problem the best known analytical method is the Hertzian theory established by Heinrich Hertz in 1882 [13]. Hertz's theory has been commonly utilized due to its reasonable accuracy in most of wheel-rail contact situations. The geometry of the contact zone and the distribution of contact pressure can be determined from this theory. Hertz's theory is based on some assumptions [33],

- The materials of the contacting solids are elastic, isotropic and homogenous and the strains are small
- Ideally smooth and frictionless surfaces
- The bodies deform like infinite half-spaces. The theory mainly applies to non-conforming contacts. A contact is said to be a non-conforming if the bodies initially meet at a point (or a line).

For tangential wheel-rail contact problem there are mainly four scholars which are mentioned often. The first treatment of rolling contact theory was done by Carter in 1926, [14]. Carter

established the first two-dimensional (2D) model to calculate the tangential forces. In 1958 Johnson extended Carter's two dimensional theory to a three-dimensional case of two rolling spheres in which the longitudinal and the lateral creepages were included, but the spin creep was not considered [15]. During 1933-2006 J.J Kalker had been introducing a number of valuable wheel-rail contact theories, which are useful to determine the wheel-rail contact tangential force as well as the spin movement between the wheel and the rail [16]. He developed two popular software's CONTACT and FASTSIM to estimate wheel-rail contact problem. Although CONTACT and FASTSIM have showed good accuracy in wheel-rail contact calculation, the computational time is often too long. In 1999, Polach introduced a model for calculating the wheel/rail creep forces [18]. Polach's fundamental idea is that the creep force is acquired by integrating the shear stress distribution over the contact zone. Polach considered friction.

The above mentioned theoretical solutions are all based on the elastic half-space approximation approach. In this study hertz normal contact theory and Polach's tangential theory are used in the analytical analysis.

2.3. Over view of wheel-rail contact conditions

When performing this study the research studies regarding adhesion loss done by different researchers (scholars) should be taken into account. Because since varying COF is considered in this study, this has a major relation to the adhesion effect on the rail.

The first research reviewed regarding this area is done in our country by Mesfin G/tsadik [19] on the "Extent of Adhesion losses in the wheel/rail contact under contaminated conditions"

This study examines the influence of several contaminants, i.e., water, mud, leaves, oil and grease on the adhesion in the wheel tread-railhead contact. In his study adhesion losses were assessed using twin disc test machine (laboratory test). The extent of adhesion over a range of slip values (0-10%) with and without contaminants is investigated. The outcome of the research is the coefficients of adhesions of each contaminants and sort out which are the worst contaminants to cause loss of adhesion. From the results highest adhesion levels are obtained in dry conditions without contaminants, which is 0.58 adhesion coefficient for slip value of 3%.

And under water condition 0.29 adhesion coefficients at 3% slip value, grease condition 0.1 maximum adhesion coefficients are obtained. An adequate braking performance demands an adhesion up to 0.09, whereas in traction, this can be up to 0.2. Under dry contact highest adhesion and higher wear debris was collected which is an indication of high wear. Moderate adhesion levels is reached within water condition which is advantageous to reduce wear and the occurrence of rolling contact fatigue defects in rails subject to high tangential forces, like in accelerating/braking sections and short-radius curves.

Under grease contact condition can lead to traction problems. Poor adhesion affects the traction while pulling away from a station and a delay is enforced the train operator will incur costs and time delay.

Limitation: As helpful as high adhesion is to railway operation, it can also have an effect on fatigue performance of the rail. The main limitation of this study is that it did not consider these effects of high adhesion. The effect of these contaminants (water and oil) on the fatigue life of the rail is not considered. If the adhesion is too high, wheel and rails can go to excessive shear stress, leading to severe wear and surface fatigue. So in the present study the effects of dry and lubricated contact conditions on the fatigue life of the rail will be presented.

In another review, K. D. VO [22], in his paper "A 3D dynamic model to investigate wheel-rail contact under High and low adhesion". In this paper high and low adhesion conditions are investigated using finite element method. A three-dimensional wheel-rail contact model is examined with an elastic-plastic material model. Rolling contact conditions consisted of high/low adhesion conditions and full slip conditions. Different values of longitudinal creepages are chosen to examine the influence of different adhesion levels on contact stresses. Low adhesion (0.28%), high adhesion (0.47%) and full slip (1.2 %). The rail head and rail gauge corner contact positions were applied in the study. The out puts of the Polach's model and the Contact software were compared with the FE method in terms of normal force, traction force and adhesion level. The FEM was found to be in good agreement with contact and Polach's theory. The researchers also considered only dry COF in the numeric calculations. The results showed that varying the adhesion condition from low to high causes a significant change to traction force

and tangential stress components. Based on the shakedown map, it was anticipated that the rail would be damaged from ratcheting response.

In another paper, K.D VO [3]. "A tool to estimate the wheel/rail contact and temperature rising under dry, wet and oily conditions"

In this paper, Finite element methods have been applied to evaluate the wheel/rail contact stress under different contact conditions. The elastic-plastic model coded in ANSYS/LS-DYNA includes a whole wheel, 680 mm of the canted rail, and sub-components of the track (rail pads, sleepers, and ballast). The three values of friction coefficient 0.4, 0.2 and 0.07 have been chosen to model dry, wet and oily environmental contacts, respectively. The ANZRI wheel and 60kg/m rail are utilized to construct the models. The wheel/rail profiles are plotted in pro Engineer and then imported to ANSYS. The wheel is set rolling on the rail under the speed of 80 km/h, and a normal load of 13KN. The FEM results obtained are presented as follows

Contact condition	Traction force	Contact pressure	Maximum shear
Dry(COF=0.4)	51.51	1167	462
Wet(COF=0.2)	25.44	1162	229
Oil(COF=0.07)	8.47	1166	77

Table 2.3-1: Results summery of contact pressure and contact shear stress.

The summary of results for different friction conditions is presented in the above table. It is concluded in this paper that the friction coefficients has minor effect on the maximum contact pressure, nevertheless the value of shear stress varies significantly to the changing of environmental conditions. In particular, the highest shear stress found in condition is 462 MPa, and it is 229 MPa, and 77 MPa in the cases of wet and oily conditions. The results found form this can help to validate the outputs of the present paper.

Limitation: The main limitation of this paper the fatigue life of the rail is not predicted. And also varying friction coefficient is not considered.

2.4. Overview of fatigue damage formation on rail

P. Hosseni Tehrani, M Saket [23], "Fatigue crack initiation life prediction of railroad" In this paper study fatigue initiation life prediction for railroad is done. Using ANSYS 11.0 software three dimensional elastic-plastic finite element model of wheel/rail contact is constructed and fine mesh technique in the contact region is used to achieve both computational efficiency and accuracy. Friction effect is included into material property of the contact element and coulomb friction model is used. The coulomb friction coefficient is assumed to be 0.3. Stress analysis is performed and fatigue damage in rail road is evaluated numerically using multi axial fatigue crack initiation model. Using the stress of vertical loading and material hardness material fatigue properties and wheel/rail contact situation on the fatigue crack initiation life is investigated. The conclusion made is that the damage accumulation rate increase as the vertical load increases. Limitation: The main limitation of this paper is that it didn't consider the varying coefficient of friction, third body materials present on rail or any environmental conditions on the rail.

U Olofsson and R. Nilsson [24] they studied the development of surface fatigue on new and 3-year old rails in a commuter railway track over a period of 2 years with and without lubrication. Four curves with radius between 303 and 616 m. Two different rail steel grades of UIC 900A grade with ultimate strength 900 N/mm^2 and UIC 1100 grade with ultimate strength 1100 N/mm^2 are used. Lubrication was applied on the high rail of one of the curves with both UIC 900A and UIC 1100 grade rail and on one of the curves with only UIC 900A grade rail. The two remaining curves were not lubricated. Both materials seemed to be similarly sensitive to crack initiation but the 1100 grade rail was more sensitive to crack propagation and also more sensitive to the formation of head check cracks showing signs after 1month of traffic. Lubrication, as expected, reduced the amount of profile change on the two lubricated curves. A less expected outcome was that lubrication also reduced the rate of crack propagation. Both the crack length and the wear depth showed low values on the lubricated rail. By using a lubricant with friction modifiers the stresses was low enough to prevent crack propagation; at the same time, the rail was hard enough to reduce the wear rate.

Limitation: The main limitation in this paper is that it is not assisted by software simulation.

2.5. Summery

The wheel/rail fatigue damage is one of the major limitations of railway transportation, thus to study wheel/rail fatigue damage and to alleviate the problems are mandatory. Numerous wheel-rail failure modes have been studied both numerically and experimentally, there still remain gaps where knowledge may be improved. And also it is difficult for rail researchers to study all failure mechanisms due to the complexity of wheel-rail contact behavior. The wheel-rail contact is complex due to contact geometry, loading condition, surface condition and third body materials present, so a great emphasis should be given to this area. The contribution of the environment and third body materials to fatigue life of rail has not been widely recognized in wheel-rail system. Furthermore the comparison of stress states under dry and lubricated contact conditions and its influence on the fatigue life of rail has not been included in the former publications. These have been found to be the main gap in the former literatures. So the primary concern for this research is fatigue wear and life prediction of rail under dry and lubricated wheel-rail contact conditions including the comparison of stress states under these contact conditions.

CHAPTER THREE: ANALYTICAL AND NUMERICAL ANALYSIS OF WHEEL/RAIL CONTACT UNDER DRY AND LUBRICATED CONTACT CONDITIONS

3.1. Introduction

Due to relatively high cost in field tests computational approach is applied in this thesis. There are two computational approaches to estimate the wheel-rail contact problems [32]. These are numerical and analytical methods. The wheel is set to roll on a straight track in this study so only the wheel tread-rail head contact is considered.

In order to investigate the extent of any damage in the wheel/rail contact, the stress states at the contact should be predicted accurately. The stresses produced at the contact are called contact stresses. In the contact zone between wheel and rail, normal and tangential loads are transmitted, due to this loads normal and tangential stress distributions are formulated [33].

The theoretical method is based on the Hertz normal contact theory to analyze the contact pressure and contact stresses at the normal contact problem. Polach's Tangential Contact theory is implemented to evaluate the tangential force (traction force).

The numerical method is done by first using the Solid works for the modeling of the 3D wheel/rail model and then by using ANSYS 15 commercial software the finite element analysis will be implemented. ANSYS software is chosen for this study based on the literatures reviewed and also the ANSYS Fatigue module has a wide range of features for performing calculations and presenting analysis results. So for this study ANSYS software is selected to analyze the fatigue life of the rail.

The main technical parameter based on the AA-LRT current operating system is given bellow for the analysis.

3.1.1. Wheel-Rail technical specifications

3.1.1.1. Wheel/rail parameters

The following are general wheel/rail parameters used for this thesis

Parameter	Value
Type of rail for main lines and depot	50 Kg/m
Length of the rail	600 mm
Type of wheel	UIC standard
Wheel diameter	≤660 mm
Maximum operation speed	70 Km/Hr.

Table 3.1-1: General wheel/rail parameters used for this thesis [25]

3.1.1.2. Applied Load

A wheel set comprises two wheels rigidly connected by a common axle. Load is proportional on each wheel. The loads listed below are based on the ERC (AA LRT) operation.

Given -Empty (Tare) load: 44 t, Axle number =6

Carrying capacity is calculated by taking average of 60kg/person and total rate of person inside of the tram.

Number of passengers	Seated	Standing	Total
Seated (AW_1)	65	0	65
Seating capacity (AW_2)	65	189	254
Overload capacity (AW_3)	65	252	317

Table 3.1-2: Carrying Capacity of AA light rail [27]

The vertical downward load is the sum of Tare load and Carrying capacity

Carrying Capacity=317*60=19.02 t

Gross load= Empty (tare) load+ Carrying capacity= 44 t+19.02 t=63.02 t

Maximum axle load= Gross load/number of axle =63.02t/6=10.5 (1 ±3%) =10.82 t

Load on wheel (F_N) = Maximum axle load/Number of wheel on axle=10.82/2=*5.41 t*

5.41*9.81*1000= *53060 N*

The maximum of the design load of the under over load condition *53060 N* is used to perform the study.

3.1.1.3. Rotational Velocity

Maximum operating speed is given 70Km/h [27]. The angular velocity of the wheel with maximum operating speed of the vehicle is:

$$\boldsymbol{\omega = \frac{V}{R_w}} \qquad 3\text{-}1$$

Where V is the maximum operation speed of the vehicle, 70Km/hr. =19.44 m/s and R_w is the principal rolling radius of the wheel, 0.33m, ω =*58.91 rad/sec*

3.1.1.4. Coefficient of friction

Usually many studies have been made by using constant COF in the analysis. However the friction coefficient on the rail surface varies significantly due to environmental conditions. And also can be contaminated by third body material present on the rail such as grease and water. Since it is hard to measure the COF, it is simply selected based on the third body materials present from figure 1-3.

- Dry wheel/rail contact condition:

For the dry condition in case of high sunshine, a thick oxide layer is formed on the rail, and the friction coefficient can be as high as 0.6-0.7. Normally 0.6 is the common one, 0.7 COF is very rare. So for this study 0.6 is selected.

- Lubricated wheel/rail contact conditions

Under lubricated contact conditions water and oil are selected as natural and artificial contaminants present in the rail surface. Water present on the rail can reduce the friction up to 0.2. And for grease present on the rail the friction coefficient is as low as 0.05.

The selected coefficient of frictions based on Figure1-3, is summarized as follows

	Conditions	Coefficient of friction (μ)
Case 1	Sunshine, dry rail	0.6
Case 2	Recent rain on rail	0.2
Case 3	Grease on rail	0.05

Table 3.1-3: Selected COF for this study

3.1.2. Hertz normal contact theory

Although Hertzian theory rests on a number of rather restrictive assumptions, it is still widely used in studying wheel-rail contact, and serves as a foundation for many tangential contact theories [12]. Two non-conforming solid bodies approaching each other must initially touch at a point, or a line. Then the surfaces will elastically compress and from an elliptical area of contact. The Hertzian theory is based on the assumption [33] given in the literature.

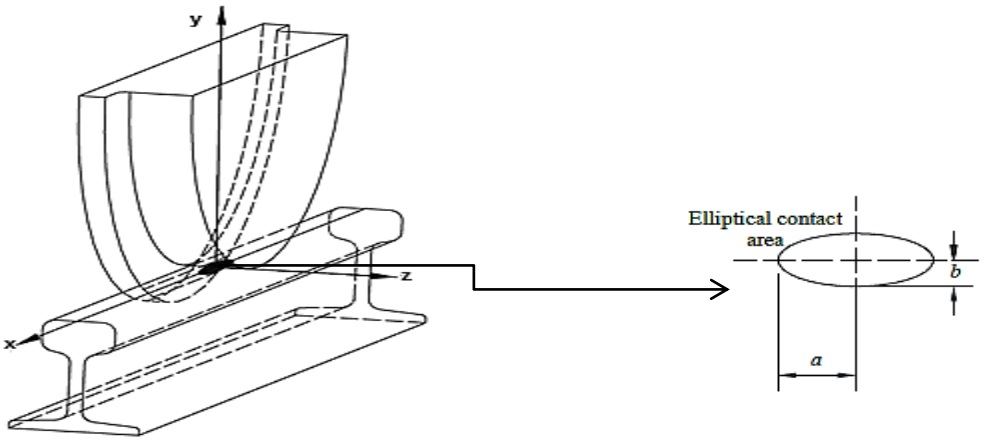

Figure 3.1-1: Hertzian Contact: the railway case [31]

3.1.2.1. Contact Area Calculation

If two bodies pressed together have different radii of curvature along the co-ordinate axes, the contact area is elliptical in shape.

The semi-minor axis 'a' and semi-major axis 'b' of the elliptical contact are calculated as follows [33].

$$ab = mn\left[\frac{3F_N}{4E^*(A+B)}\right]^{\frac{1}{3}} \qquad 3\text{-}2$$

Based on the wheel-rail configuration, the Geometric constants A and B which depends on the geometric properties of the two bodies are calculated based on the wheel/rail curvature combinations.

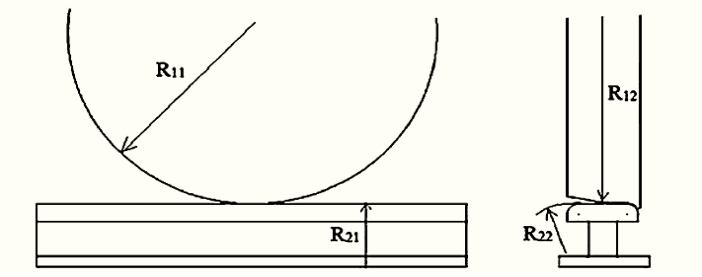

Figure 3.1-2: Wheel-rail configuration showing different principal relative radii of curvature [33]

The principal rolling radii of the wheel R_{11}=330 mm,

The principal transverse radii of the wheel $R'_{12}=\infty$

The principal rolling radii of the Rail $R'_{21}=\infty$

The principal transverse radii of the rail R_{22}=300mm,

$$\mathbf{A+B}=\frac{1}{2}*\left(\frac{1}{R_{11}}+\frac{1}{R'_{12}}+\frac{1}{R_{22}}+\frac{1}{R'_{21}}\right) \quad 3\text{-}3$$

$$A+B=3.2/m$$

$$\mathbf{A-B}=\frac{1}{2}\sqrt{\left(\left(\frac{1}{R_{11}}-\frac{1}{R'_{12}}\right)^2+\left(\frac{1}{R_{22}}-\frac{1}{R'_{21}}\right)^2+2\left(\frac{1}{R_{11}}-\frac{1}{R'_{12}}\right)\left(\frac{1}{R_{22}}-\frac{1}{R'_{21}}\right)\cos(2\varphi)\right)} \quad 3\text{-}4$$

The angle between the radius of the wheel and rail φ is called angle of attack (yaw rotation). This is the angle of orientation difference of the principal axes (planes) of curvature of two bodies. For this case $\varphi=(\pi/2)$

$$A-B=0.1515/m$$

The parameters m and n are Hertz coefficients and they are given as a function of the angle θ (0^0-90^0), where θ, is given as

$$\cos(\theta)=\frac{A-B}{A+B} \quad 3\text{-}5$$

$$\cos(\theta)=0.047,\ \theta=87.3$$

Then by using linear interpolation method the value of m and n is obtained from the following Hertz coefficient table

$$m=1.033,\ n=0.97$$

The equivalent Young's modulus (E*) given by;

$$\frac{1}{E^*} = \left[\frac{1-\nu_1^2}{E_1} + \frac{1-\nu_2^2}{E_2}\right] \quad 3\text{-}6$$

Where, $E_{1,2} = 210\ GPa$ and $\nu_{1,\,2}$ =0.3 being the elastic moduli and Poisson ratios of the bodies in contact respectively.

$E^* = 115.38\ GPa$

Then finally the major and minor semi-axis will be

$$a = m\left[\frac{3F_N}{4E^*(A+B)}\right]^{\frac{1}{3}} \quad 3\text{-}7$$

$a = 6.2\ mm$

$$b = n\left[\frac{3F_N}{4E^*(A+B)}\right]^{\frac{1}{3}} \quad 3\text{-}8$$

$b = 5.83\ mm$

3.1.2.2. Contact Pressure

The integration of the contact pressure over the contact patch must be due to the total applied force due to static equilibrium. The pressure acting over the elliptical contact area is given by

$$P(x,y) = P_0\sqrt{1 - \frac{x^2}{a^2} - \frac{y^2}{b^2}} \quad 3\text{-}9$$

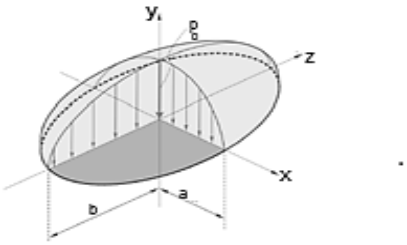

Figure 3.1-3: Contact Pressure distribution [30]

The maximum contact pressure (P_0) given by,

$$\mathbf{P_0 = \frac{3F_N}{2\pi ab}} \qquad 3\text{-}10$$

P_0= *701.2 MPa*, since the contact pressure is less than the Ultimate strength of the rail (888 MPa) given in table 3-5 the above considered parameters are safe for further operation.

3.1.3. Tangential contact theory

The wheel-rail contact occurs in combination of sliding and rolling regime, since there is usually a velocity difference between wheel rolling speed and vehicle running speed. The ratio between the velocity (translational velocity) difference and the rolling speed (rotational velocity) is defined as creep, ($\boldsymbol{\xi}$),

In this study since the wheel tread-rail head on a straight track contact is considered, only longitudinal creep is considered. The longitudinal creep is given by [32]:-

$$\boldsymbol{\xi = \frac{\omega R - V}{\frac{\omega R + V}{2}}} \qquad 3\text{-}11$$

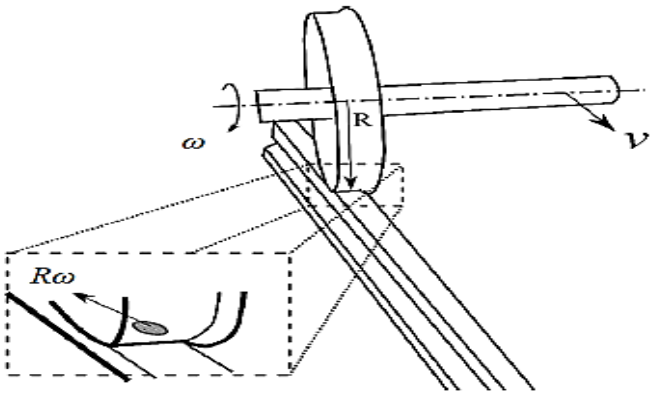

Figure 3.1-4: Illustration of translational and rotational velocity of the wheel set [32]

Where $\boldsymbol{\omega}$ is rotational velocity from Eqn. 3-1 (58.92 rad/sec), R=0.33m and V is the translational velocity (70Km/hr.=19.44 m/sec) so from this $\boldsymbol{\xi}$=0.001, is the longitudinal creepage for this study.

Due to this creep, the contact areas are divided into stick and slip regions. When creep is zero, the motion is pure rolling motion and the stick region covers the whole contact area. No tangential force is transmitted under pure rolling.

When a tangential force starts to be transmitted, a slip region appears in the contact patch. With increasing creep, the slip region increases and the stick region decreases in size, resulting in a rolling-sliding contact. When creep is great enough, the stick region disappears leading to gross slip. This usually occurs for contacts located on the flange of an outer wheel and on the gauge corner of an outer rail in curves. The maximum tangential force is limited by the friction force available between the two surfaces [16]. In rolling contact, the relationship between the traction force and creepage is illustrated in figure below.

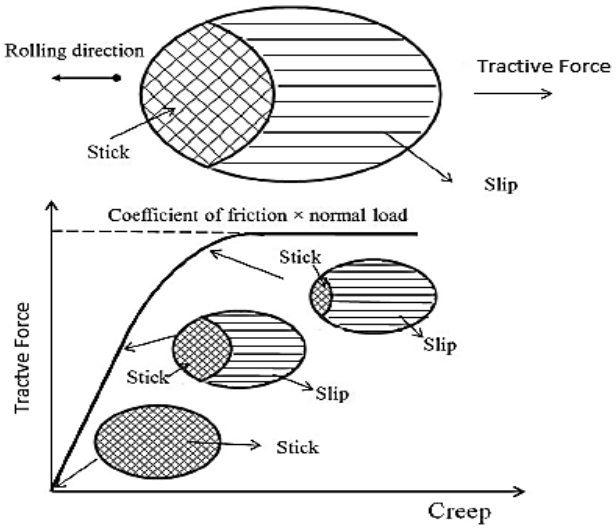

Figure 3.1-5: Relationship between traction and creep in the wheel/rail contact [26]

The traction/creep curve is dramatically affected by the presence of a third body layer in the wheel/rail contact.

3.1.3.1. Polach's tangential theory

The tangential force is known as traction, which ultimately propels the wheel along the rail, due to friction [7].Here the main aim is to calculate the tangential force. Different traditional theories

have been summarized in the literature; from those the selected one for this analysis is the Polach's theory.

Polach's theory is three dimensional contact model based on the integration of shear stress in the contact interface in order to compute the traction force. The proposed method is based on hertz elliptical contact area. It assumes that the elliptical contact is divided to Stick and slip regions. Polach's theory also considered the relationship between creepage and Coefficients of friction [18].

$$\mathbf{Q = \iint \tau \, dx \, dy} \qquad 3\text{-}12$$

The maximum tangential stress at any arbitrary point is

$$\boldsymbol{\tau_{max} = \mu\sigma} \qquad 3\text{-}13$$

where $\boldsymbol{\sigma}$, is the normal stress

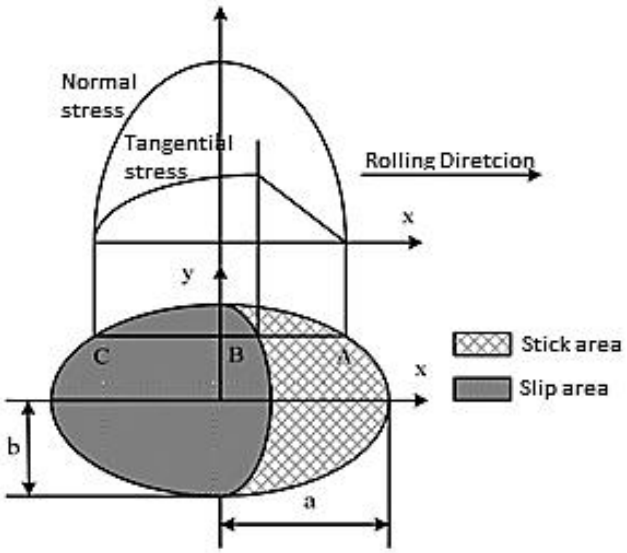

Figure 3.1-6: Polach's tangential contact theory [18]

From the figure, we can observe that as soon the tangential stress achieves its maximum value, sliding phenomena will happen.

The tangential traction force is described by Polach O. Only longitudinal creep is considered in this case, since the wheel is set to move on a straight line having wheel tread-rail head contact.

$$\mathbf{Q} = \frac{\mathbf{2\mu F_N}}{\boldsymbol{\pi}} \left(\frac{\boldsymbol{\varepsilon}}{\mathbf{1+\varepsilon^2}} + \mathbf{arctan\varepsilon} \right) \quad 3\text{-}14$$

Where

- F_N-wheel load
- μ is coefficient of friction
- ε is gradient of the tangential and is obtained by

$$\mathcal{E} = \frac{\mathbf{2}}{\mathbf{3}} \frac{\mathbf{G\pi abC_{ij}}}{\mathbf{N\mu}} \quad 3\text{-}15$$

G is the modulus of rigidity given by,

$$\mathbf{G} = \frac{\mathbf{E}}{\mathbf{2(1+v)}} = \mathbf{79.61}\ \boldsymbol{GPa} \quad 3\text{-}16$$

And C_{jj} is the longitudinal creepage coefficient given by, the longitudinal creepage is calculated as 0.001.

$$\mathbf{C_{ij}} = \mathbf{C_{11}} * \boldsymbol{\xi} \quad 3\text{-}17$$

C_{11} is Kalker's creep coefficient, it is found from the Kalker's creep coefficient table (Appendix).

For the ratio b/a=0.9 and for v= 0.25 C_{11}= 4.22, $C_{jj} = 4.22 * 0.001 = 0.00422$

CASE 1: Dry wheel-rail contact condition, μ=0.6

$$\mathcal{E} = \frac{2}{3} \frac{G\pi abC_{jj}}{N\mu} = 5.93$$

$$Q = \frac{2\mu F_N}{\pi} \left(\frac{\varepsilon}{1+\varepsilon^2} + \arctan\varepsilon \right) = 31.6\ KN$$

CASE 2: Water lubricated condition, μ=0.2

$Q = 10.54\ KN$

CASE 3: Grease lubricated condition, μ=0.05

$Q = 2.64\ \ KN$

The above results can be summarized in the following graph. Under the same longitudinal creepage, it can be seen from the graph that under dry contact condition, when the friction is high the traction force also increases. This is 31.6 KN, and under water lubricated contact the traction force significantly reduces to 10.54 KN. Which is further reduced to 2.64 KN under grease lubricated contact. The result found here can be validated with the literature [3].

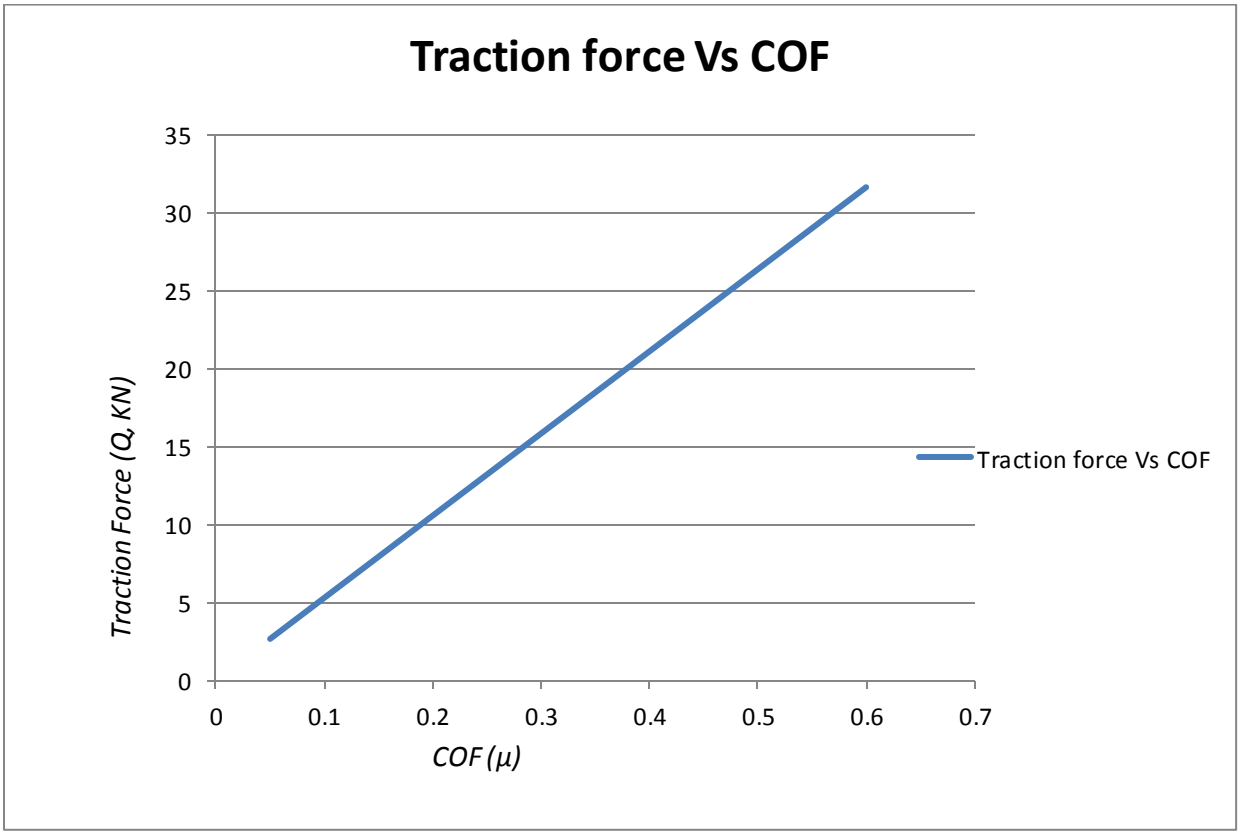

Figure 3.1-7: Traction force Vs. Coefficient of friction

Result summery of the Analytical analysis

Contact conditions	Hertz normal contact theory	Polach's tangential contact theory
	Max. Contact pressure(MPa)	Traction force(KN)
Case 1(Dry)	701.2	31.6
Case 2(Water)	701.2	10.54
Case 3(Grease)	701.2	2.64

Table 3.1-4: Result summery from the Analytical calculations

3.2. Numerical Analysis

In order to build a realistic model of wheel/rail contact problem a three dimensional model is implemented. This model is able to calculate the three dimensional stress responses in the contact region as well as includes both material and geometric nonlinearity.

Finite element method is developed to analyze the wheel-rail contact problem. The finite element analysis is validated to overcome the limitations of the theoretical tools [30]. Different software products are used to perform the numerical which include;

- SOLID WORKS 2013
- ANSYS R15.0

3.2.1.1. Main Wheel/rail geometry

The standard rail and wheel types used in the Addis Ababa Light Rail Transit Project system are chosen. The rail type used in the present study is as per Chinese national standard, which is TB10082-2005(50Kg/m). And 660mm diameter wheel is as per the international union of rail way (UIC) standard is used.

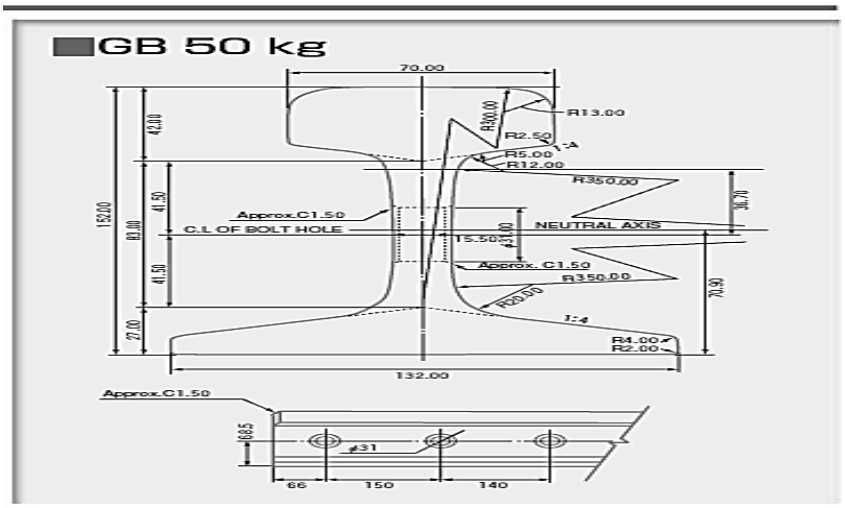

Figure 3.2-1: Type of rail: TB10082-2005(50Kg/m) [25]

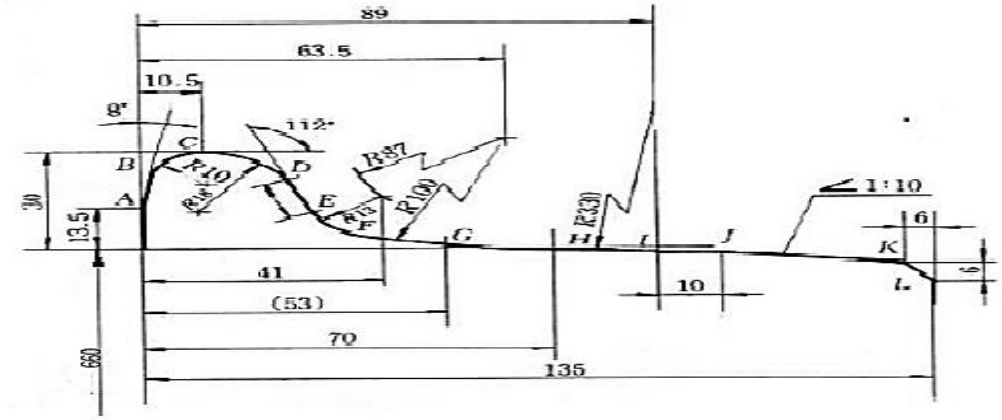

Figure 3.2-2: Wheel profile for AA-LRT based on UIC standard wheel

3.2.2. Wheel and Rail Profiles

The wheel/ rail part and assembly modeling is done using the software Solid Works. The wheel is set to roll on a straight line, only wheel tread –rail head contact is considered. The length of the rail is taken 600mm, which is an average distance between two sleepers.

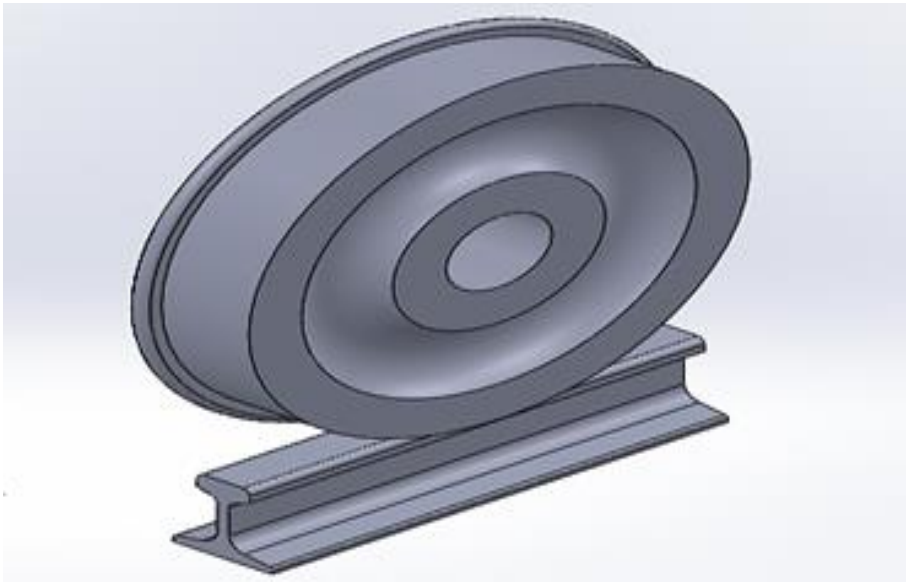

Figure 3.2-3: Wheel/rail assembly by Solid works

3.2.3. Structural Analysis

The assembly of wheel/rail contact generated by the Solid works is exported to ANSYS 15.0 commercial software. The finite element method is applied using static structural analysis in ANSYS. Finite element method is mathematical modeling tool involving discretization of a continuous domain using building-block entities called finite elements connected to each other by nodes for once and moment transfer [30]. ANSYS solves governing differential equations by breaking the problem into small elements. Static structural analysis is mainly selected for this analysis, since the effect of static friction is greater compared to dynamic effects, in order to include these effects. And also the static structural analysis is used to determine the stresses and fatigue response of structures under applied load that do not induce significant inertia and damping effect. Static analysis is used instead of explicit (dynamic) to avoid elastic wave and vibration noise in stress distribution results.

All the theoretical tools account for linear elastic material properties. The theoretical (classical) theories are based on the elastic half-space assumptions, so in order to validate the FEM results first FEM analysis will be made under elastic wheel/rail material properties. To approve the accuracy of the software responses, the study should be reduced based on elasticity assumption

of the hertz theory (frictionless and elastic material property). From the [32] if the FEA is accepted for elastic material property then it can be acceptable for elastic-plastic analysis. Then after the FE analysis of elastic-plastic material model will be utilized. Various engineering investigations can be performed by means of bi-linear elastic-plastic material model such as fatigue and effect of the plastic deformation [33]. So in order to include these effects a bi-linear elastic-plastic material model is mainly implemented in this study.

3.2.3.1. Mechanical Properties

The material property of rail used in AA LRT is U71Mn, which is equivalent to R260Mn and its mechanical property are discussed in accordance to EN 13674-1:2011(E) [25]. And the material type of the wheel used in AA-LRT is steel categories of EN 13262: ER9 [26].The mechanical properties are discussed below:

- **The elastic material property**

ITEM No	Mechanical property	Rail	Wheel
1	Steel Grade	U71 Mn	ER9
2	Poison's ratio	0.3	0.3
3	Young's Modulus (GPa)	210 GPa	210 GPa
4	Density	7800 Kg/m^3	7800 Kg/m^3
5	Ultimate tensile strength(MPa)	880 MPa	900 MPa

Table 3.2-1: Material Property of wheel and rail [25, 26]

- **Elastic-Plastic material property**

From the mechanics of material point of view, the contact between the rail and wheel is highly non-linear in its nature. So the stress and fatigue life values at the contact zone are obtained using elastic-plastic material model.

A bi-linear isotropic hardening property is used in the rail material. When a material deforms under cyclic loading materials undergo cyclic hardening, isotropic hardening identifies this effect whereby the yield space dilates with the number of cycle.

Item No.	Material Property	Rail
1	Yield strength	540 MPa
2	Tangent modulus	21 GPa

Table 3.2-2: Bi-linear material property for rail [25, 29]

Tangent modulus is equivalent to Young's Modulus, in describing behavior of material that has been stressed beyond elasticity. When a material is plastically deformed there is no longer linear relationship between stress and strain. The slope of that curve is Tangent modulus.

3.2.3.2. Wheel-Rail Contact

Surface to surface contact is applied; one of the surfaces is selected as target and the other one as the contact one. The wheel and rail surfaces are chosen as contact and target surfaces respectively.

Frictional type contact is implemented, and the selected frictions coefficients under dry, water-lubricated and grease lubricated conditions are applied.

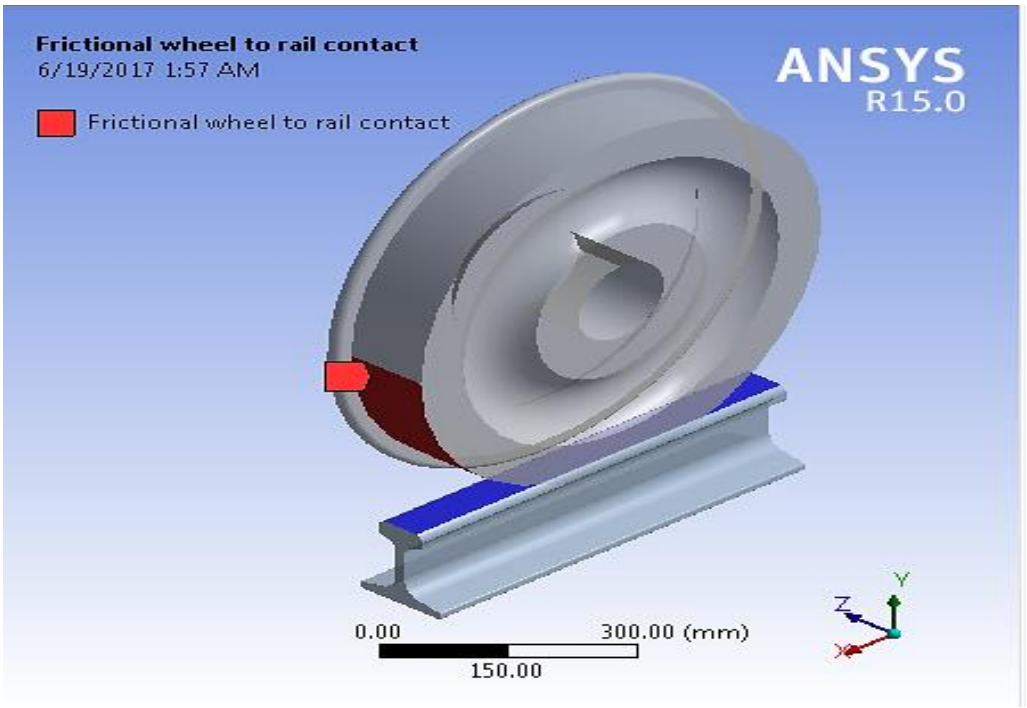

Figure 3.2-4: Frictional Wheel/rail contact condition

3.2.3.3. Meshing

Element discretization is a critical step of modeling section in the FE analysis. The strategy of meshing significantly influences the accuracy of the results and the duration of simulation.

The mesh is favored in order to obtain accurate stress results. Due to this a fine mesh (5*5 mm) is generated at the contact surface and medium mesh method is applied for those regions furthest from the contact surface. In the present work a total of 73,700 elements and 127,053 nodes are formed.

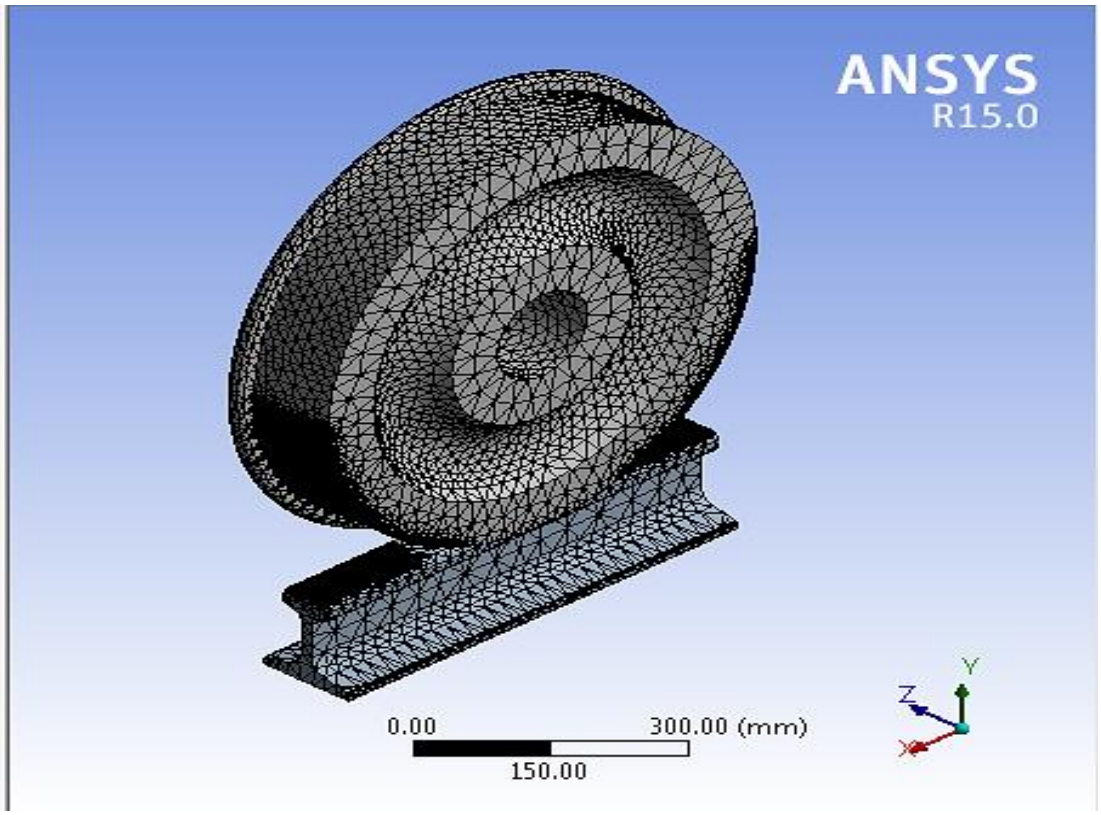

Figure 3.2-5: Wheel/rail mesh

3.2.3.4. Boundary and loading Conditions

The total vertical load applied to the wheel was calculated in the previous section, which is 53.06 KN. The center of the wheel is the location of the load applied. And also the effect of gravitational load is considered in the simulation.

The boundary conditions are applied to the bodies in order to restrict undesired displacements of the bodies in the analyses. A fixed boundary condition is applied to the rail. The base and sides of the rail is fully constrained, which is not translated or rotated to any direction (x, y, z). The wheel is free along the loading direction (-y direction) to observe the effect of load over the assembly model and is fully constrained in all the other directions. The wheel is set to roll on the rail given 58.92 rad/sec angular velocity.

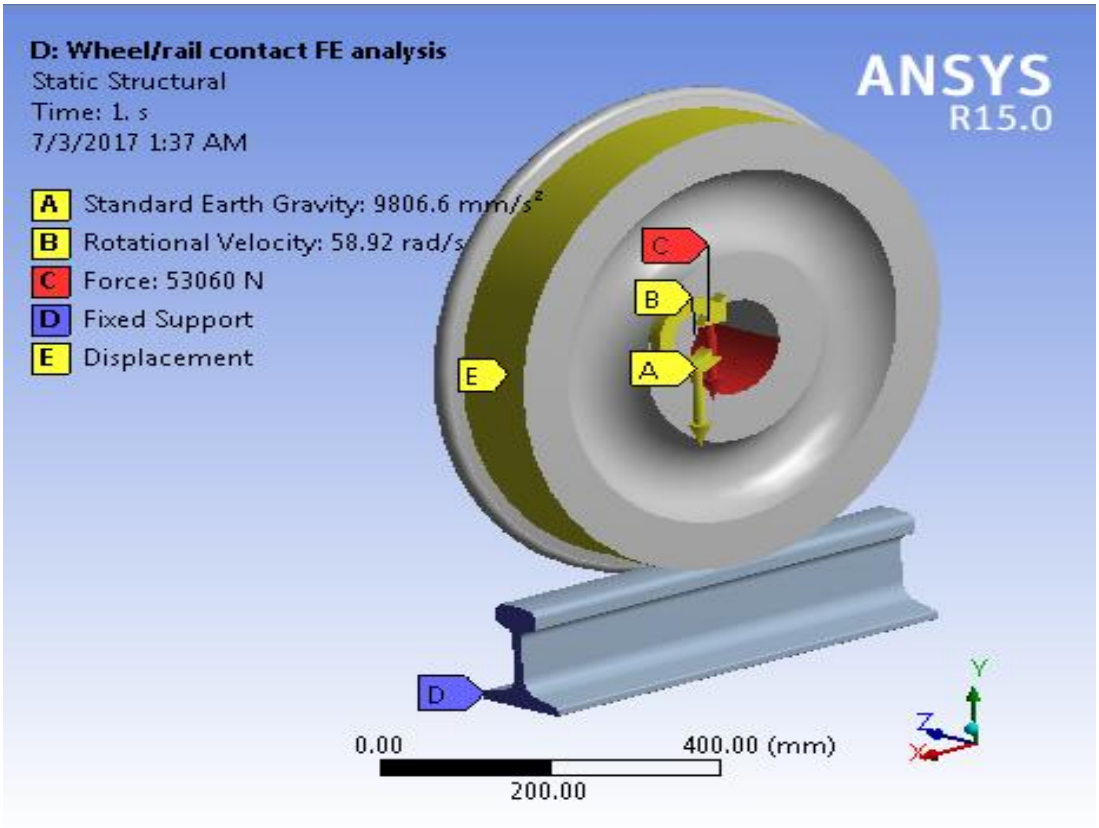

Figure 3.2-6: Loading and boundary condition using ANSYS

3.2.4. Fatigue Analysis

The objective of this analysis is to evaluate the fatigue life of the rail. Wheel/rail contacts accompanied by very high local stresses, which are repeated a large number of times cause contact fatigue. A fatigue failure constantly starts at a local discontinuity like a crack, notch or other zone of stress concentration areas [27].

Fatigue Analysis has three main methods, strain life, stress life and fracture mechanics; the first two being available within the ANSYS Fatigue Module [27]. Stress life approach used this thesis.

3.2.4.1. Stress life fatigue analysis

It is mainly concerned with the total life and does not distinguish between initiation and propagation. Stress life is based on S-N (Stress-cycle) curves. In terms of cycles, stress life has

traditionally dealt with relatively high numbers of cycles and therefore addresses high cycle fatigue (HCF), greater than 10^5 cycles inclusive of infinite life [27]. In this study the following input decision methods are selected for the analysis:-

- Loading type: - Loading is of constant amplitude, zero-based -apply a load then remove it, a load ration of 0 (load ratio is defined as the ratio of the second load to the first load). Loading is proportional since only one set of FE result is needed [28].

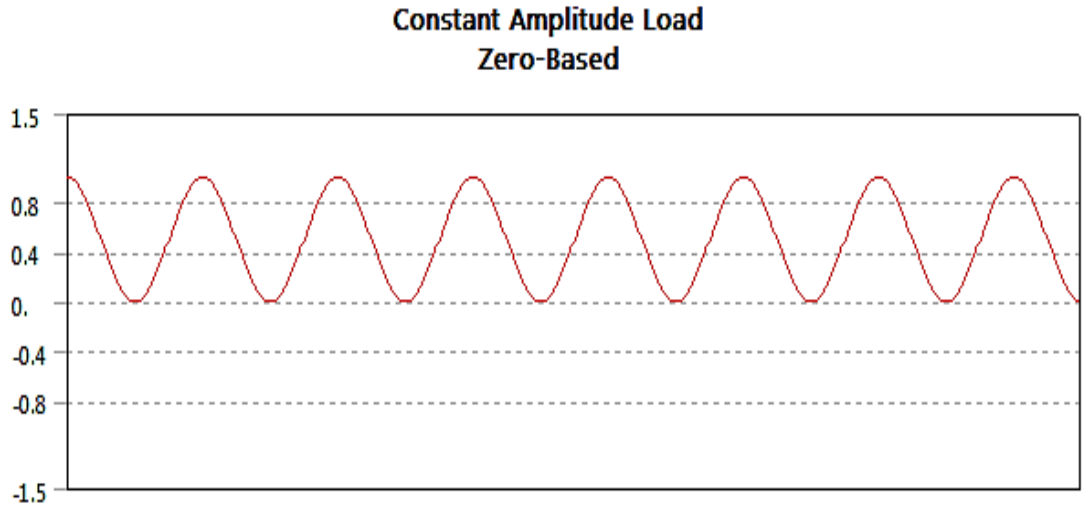

Figure 3.2.4-1: Zero –based amplitude load and Goodman theory

- Mean stress correction factor: - Since the loading is zero based, mean stress exists and is accounted for by using a mean stress correction. In order to consider the mean stress effects. Gerber approach is selected. Most experimental data fall between the Goodman and Gerber theories with Soderberg theory being overly conservative [28]. And Geber theory is usually a good choice for ductile materials. Gerber theory is given by the equation[28]

$$\sigma_{Alternating} = S_{endurance\ limit}\left(1 - \frac{\sigma_{mean}}{S_{ultimate\ strength}}\right)^2 \qquad 3\text{-}18$$

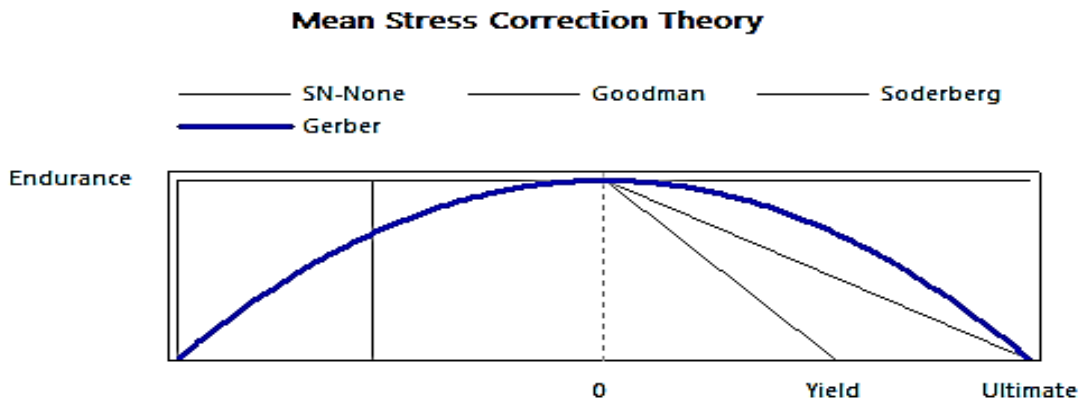

Figure 3.2.4-2: Gerber's mean stress correction theory

CHAPTER FOUR: RESULTS AND DISCUSSION

4.1. RESULTS

This section presents the detailed normal and tangential stress distributions between wheel/rail contact and fatigue analysis of rail results obtained from the finite element analysis using ANSYS. As mentioned in the procedure, first by using linear-elastic material properties of wheel and rail the results of FEA will be validated for further complex analysis. Then effect of varying friction coefficient under the three cases (dry contact, water lubricated and grease lubricated contact conditions) will be analyzed on the normal and tangential stress distribution using the elastic-plastic material property. Finally the fatigue analysis and life prediction of the rail under the three cases (dry, water lubricated and Grease lubricated contacts) is performed.

4.1.1. Frictionless contact with Linear Elastic Material property

4.1.1.1. Contact Pressure

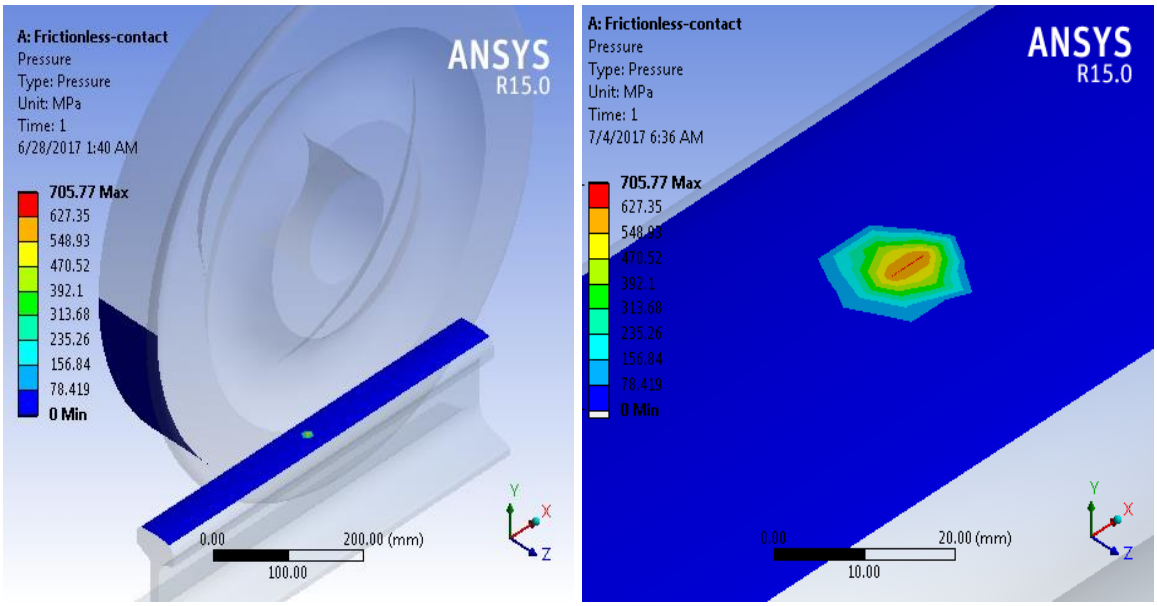

Figure 4.1-1: contact pressure under frictionless, linear elastic material property

The maximum contact pressure found using Finite element method in ANSYS is *701.5 MPa*. And from the Analytical calculation of Hertz normal contact theory the maximum contact pressure was found *700.1 MPa*.

The percentage deviation is given by

$$\% \text{ deviation} = \frac{705.77 - 701.2}{705.77} * 100\% = 0.65\ \%$$

From the, it is seen that the result of maximum contact pressure found Finite element analysis using ANSYS is in good agreement with the analytical results found using Hertz normal contact theory. As it can be seen from the result the contact area is also elliptical contact. So the proposed FEA can be further used to analyze the more complex stress and fatigue analysis under elastic-plastic analysis.

4.1.2. Frictional wheel/rail contact with elastic-plastic material property

In this section the results of stress using Finite element simulation on ANSYS are presented. Here elastic-plastic material property is used. The bi linear isotropic hardening (plastic) material property of the rail is included, which helps in including the plastic response of the rail as well. The analysis is done for the three wheel/rail contact cases under varying COF values. For dry (μ=0.6), water lubricated (μ=0.2) and grease lubricated (μ=0.05).

4.1.2.1. Contact pressure distribution

In this section the maximum contact pressure between wheel and rail is presented under dry, water lubricated and grease lubricated contact conditions are presented.

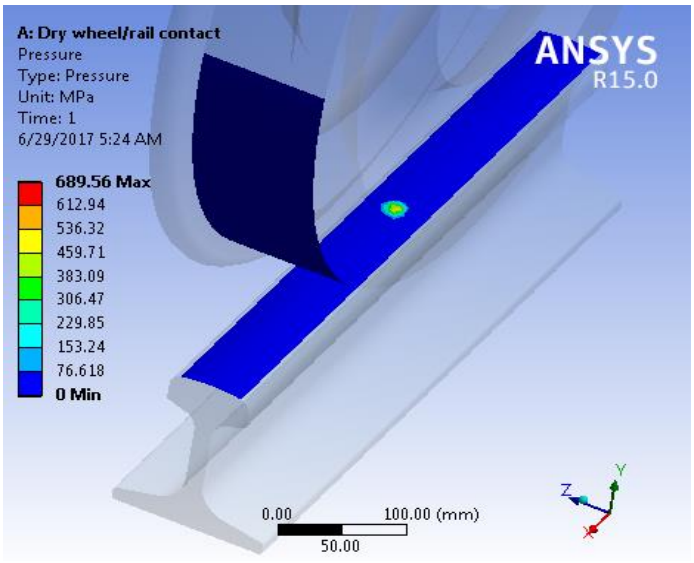

(a)

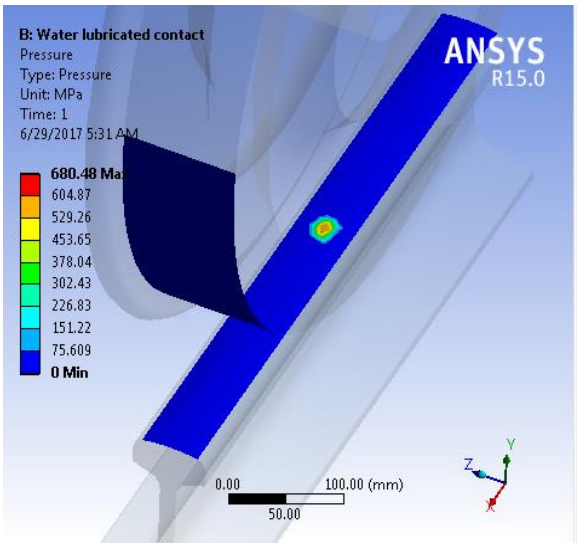

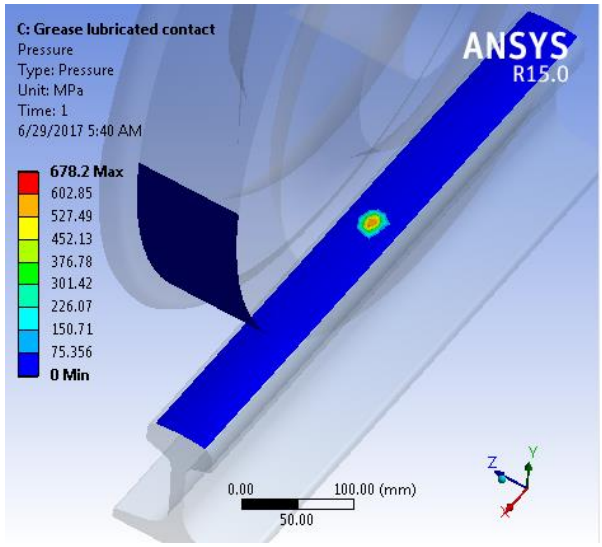

(b) (c)

Figure 4.1-2:Maximum Pressure distribution under (a) dry contact (b) water lubricated and (c) grease lubricated contact conditions

As it is seen from the results the contact pressure under dry contact (*689.56 MPa*), water lubricated (*680.48 MPa*) and grease lubricated contact is *678.2 MPa*.

4.1.2.2. Tangential contact stress distribution

4.1.2.2.1. Von-Misses Stress

Von Misses stress distribution across the wheel-rail contact interface under the three cases is presented below: Section plane feature is used to show the contact patch and display the results clearly, by cutting the model into two.

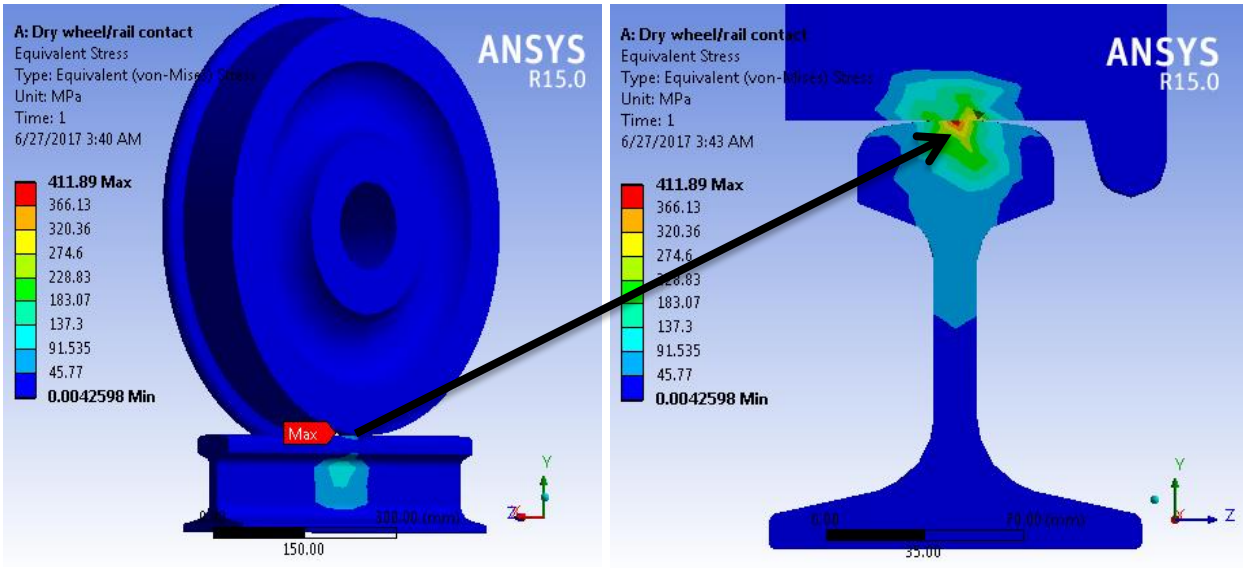

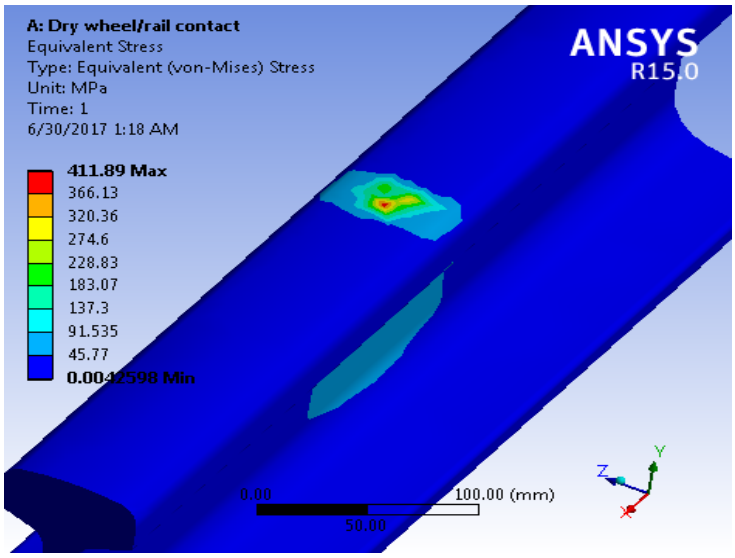

(a)

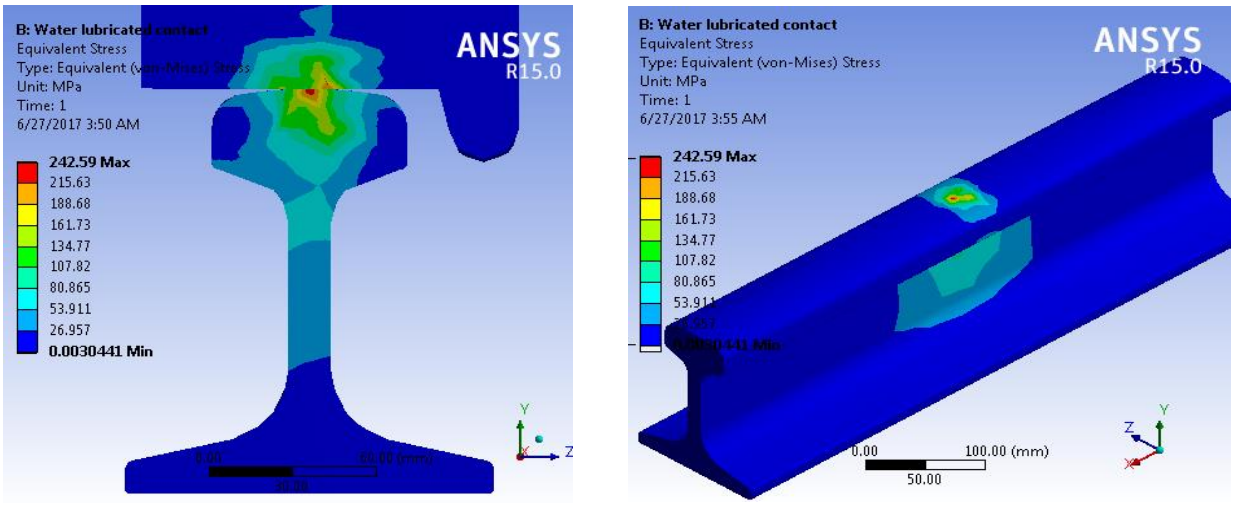

(b)

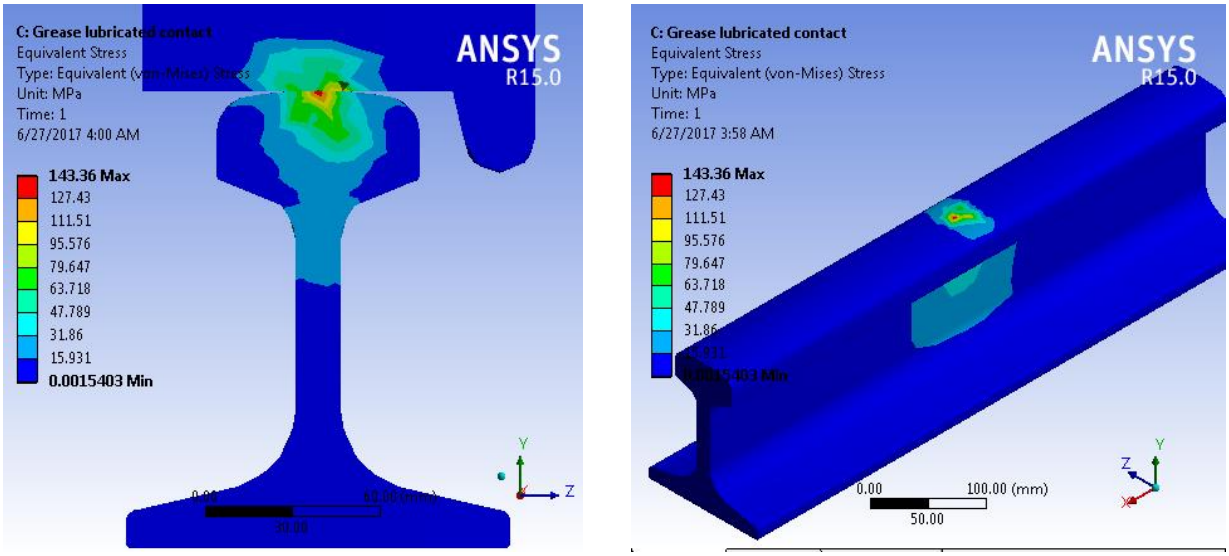

(c)

Figure 4.1-3: Von-misses stress distribution under (a) dry contact (b) water lubricated contact (c) grease lubricated contact condition

It is observed that at the inside of the rail and wheel stresses are higher in comparison to the other bulk material due to the contact between wheel and rail. The value spread over a small area of contact at the interface .It is observed that the contact stresses are maximum over a small area of contact between the rail and wheel.

From the results seen high Von-misses stress occurs under dry contact condition (*411.89 MPa)* and the stress distribution is reduced to *242.59 MPa* under water lubricated and to *143.36 MPa* under Grease lubricated contact conditions.

4.1.2.2.2. Maximum Shear Stress

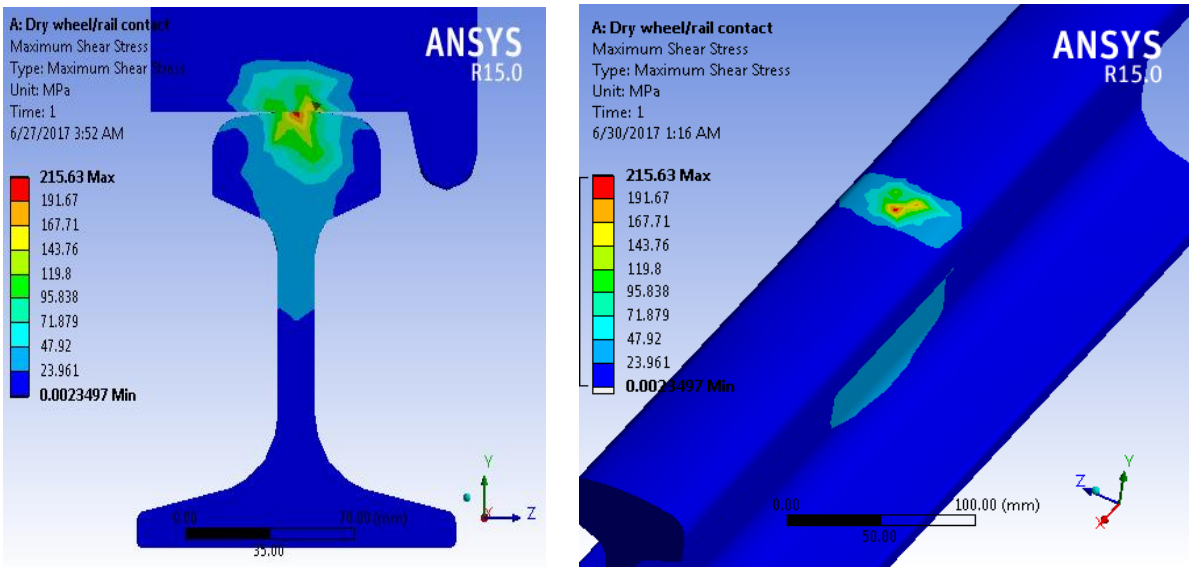

(a)

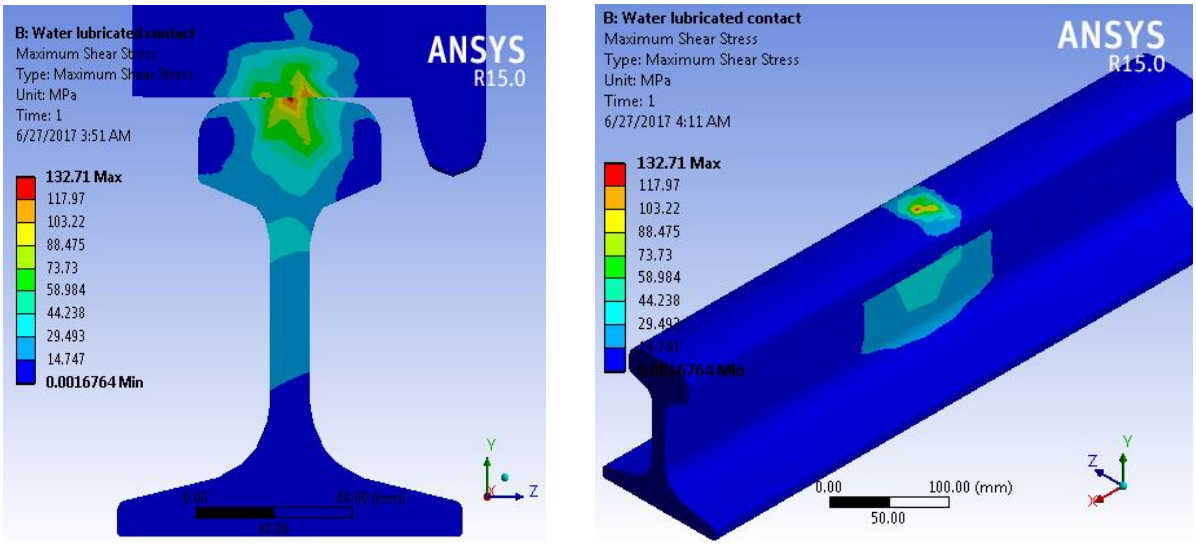

(b)

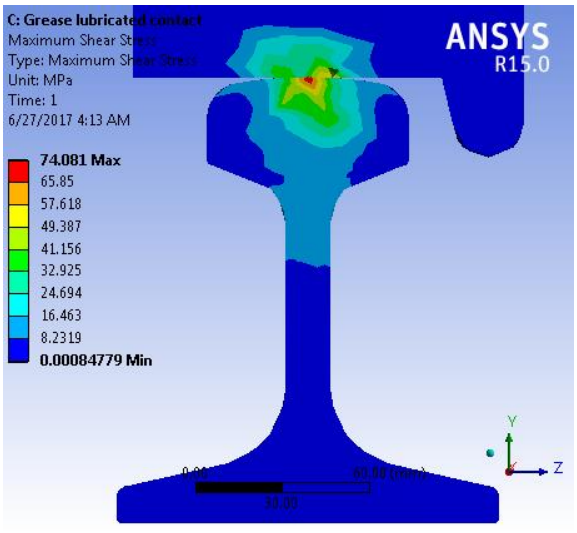

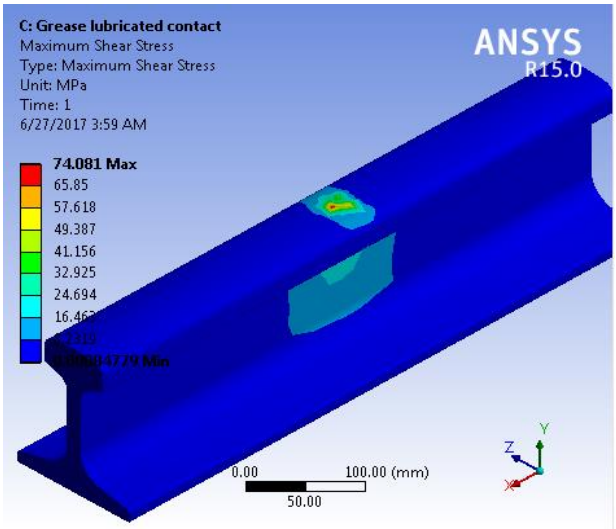

(c)

Figure 4.1-4: Maximum shear stress distribution under (a) dry contact (b) water lubricated contact (c) Grease lubricated condition

The maximum shear stress found is shown in the figures above. The highest maximum shear stress value *215.63 MPa* is found under dry wheel/rail contact condition. The values decrease to *132.71 MPa* in water lubricated contact condition and to *74.081 MPa* in Grease lubricated contact.

4.1.3. Fatigue calculations

4.1.3.1. Fatigue Life

Fatigue life is the number of cycles to failure at a specified stress level. Fatigue life can be over the whole model or scooped just like any other contour result. The following figure shows the contours for the fatigue life of the rail obtained under three cases.

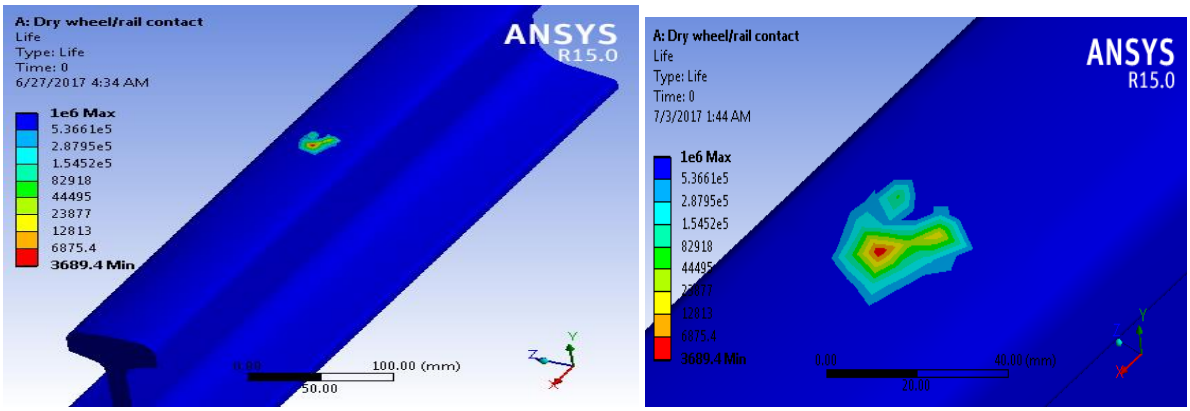

(a)

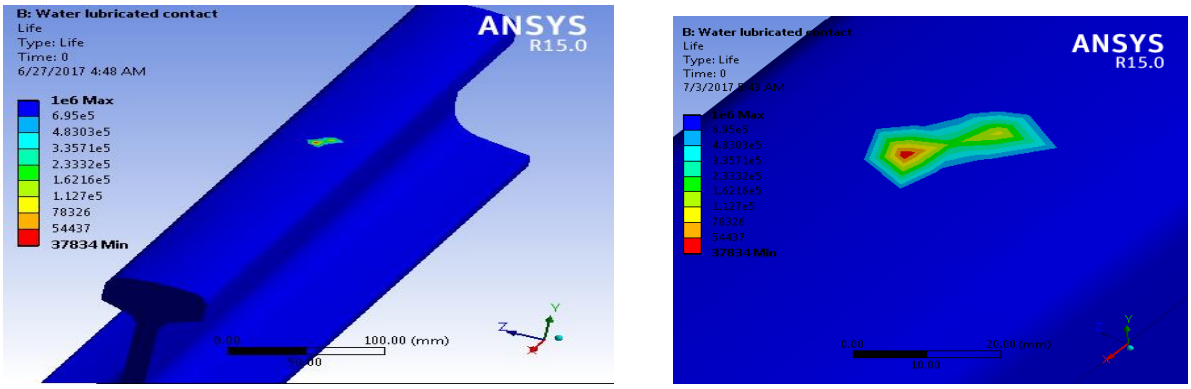

(b)

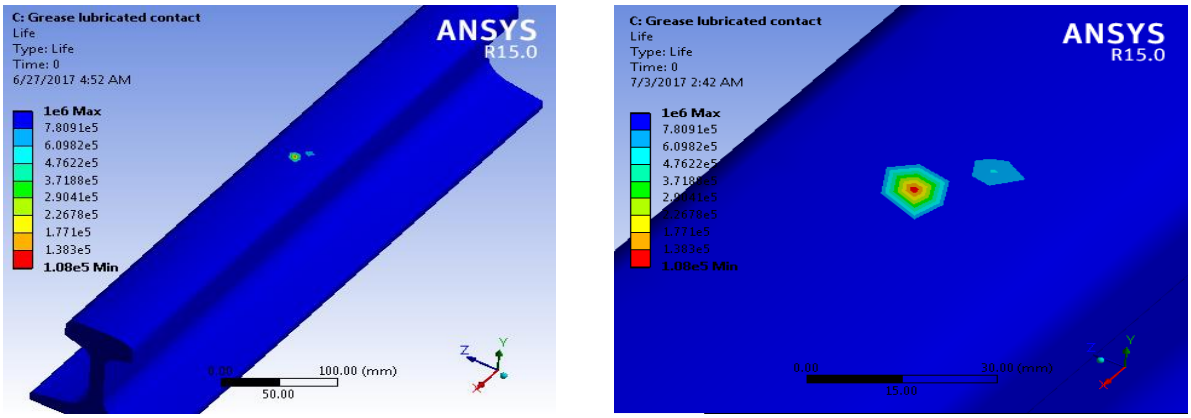

(c)

Figure 4.1-5: Fatigue life of rail under (a) dry contact (b) water lubricated and (c) Grease lubricated condition

The results above show the fatigue life the rail under the three wheel/rail contact conditions. The rail has maximum life cycle of $1*10^6$ for all the three cases. But the minimum fatigue life varies. The minimum fatigue life tells that the rail will fail if the number of cycle is greater than the minimum fatigue life at that location.

The minimum fatigue life under dry contact is *3689.7 cycles,* this value increases under water lubricated contact condition *37834 cycles* and it is $1.08e^5$ *cycles* under grease lubricated contact. The increase in minimum life cycle shows that the rail has more life cycles under water and grease lubricated before it fails compared to the dry contact condition.

4.1.3.2. Damage

Fatigue damage is a contour plot of the fatigue damage at a given design life. Fatigue damage is defined as the design life divided by the available life.

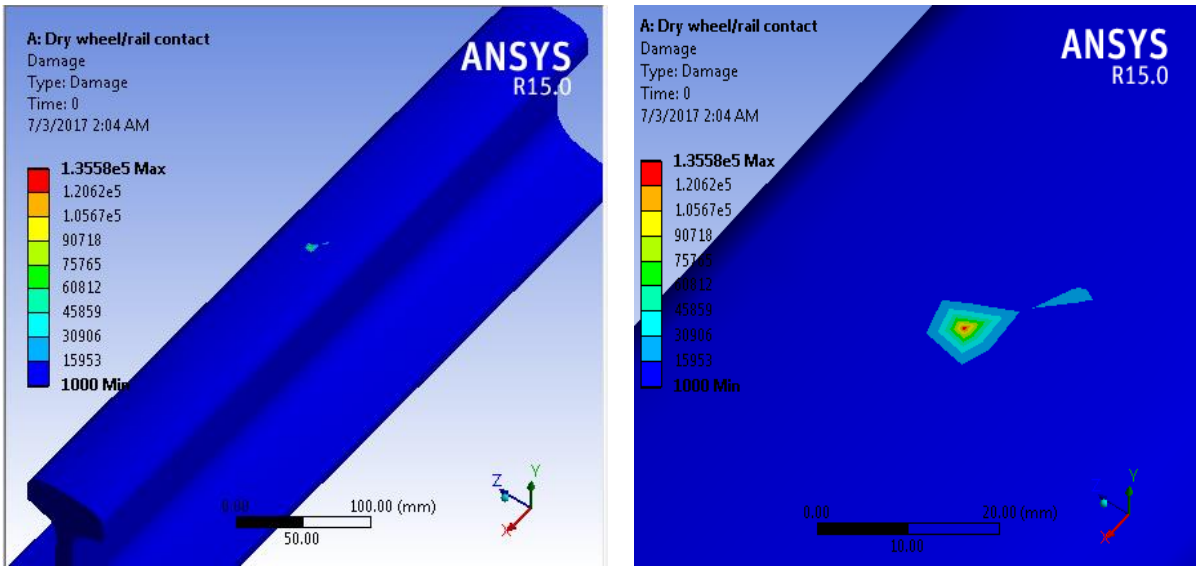

(a)

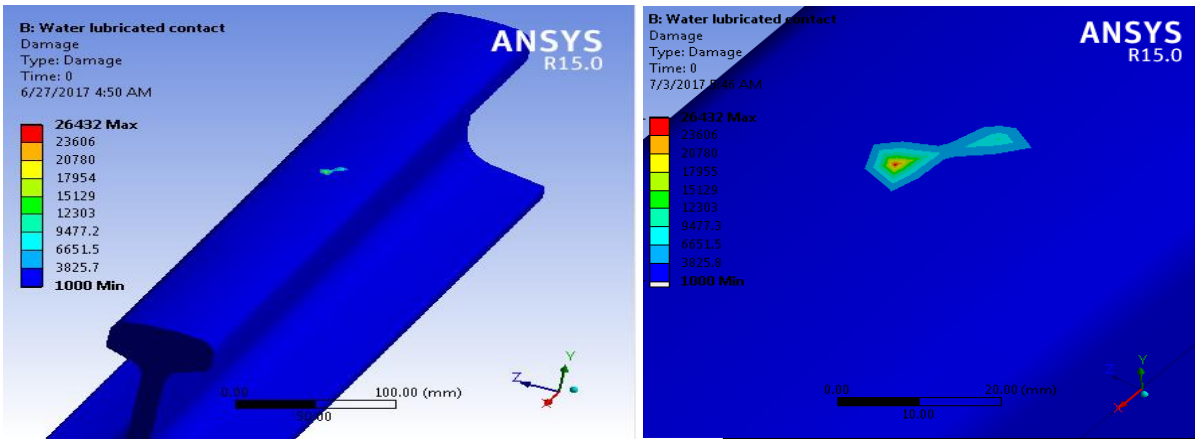

(b)

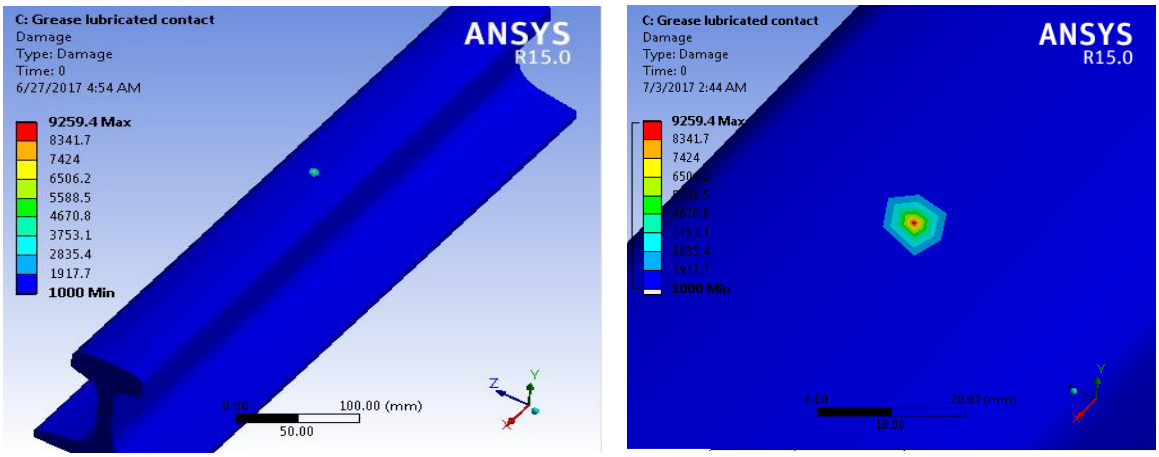

(c)

Figure 4.1-6: Damage of rail under (a) dry contact (b) water lubricated contact and (c) grease lubricated contact conditions

The higher values of damage are in consonance with the location of minimum value of the life on the rail. It can be seen that the damage formation is also higher under dry contact condition compared to water and grease lubricated conditions.

4.1.3.3. Equivalent Alternating stress

This value is unique for stress life method. In a stress life fatigue analysis SN curve is needed to relate the fatigue life to the stress states. This value is based on the mean stress correction of Gerber's method, given in equation 3-18.

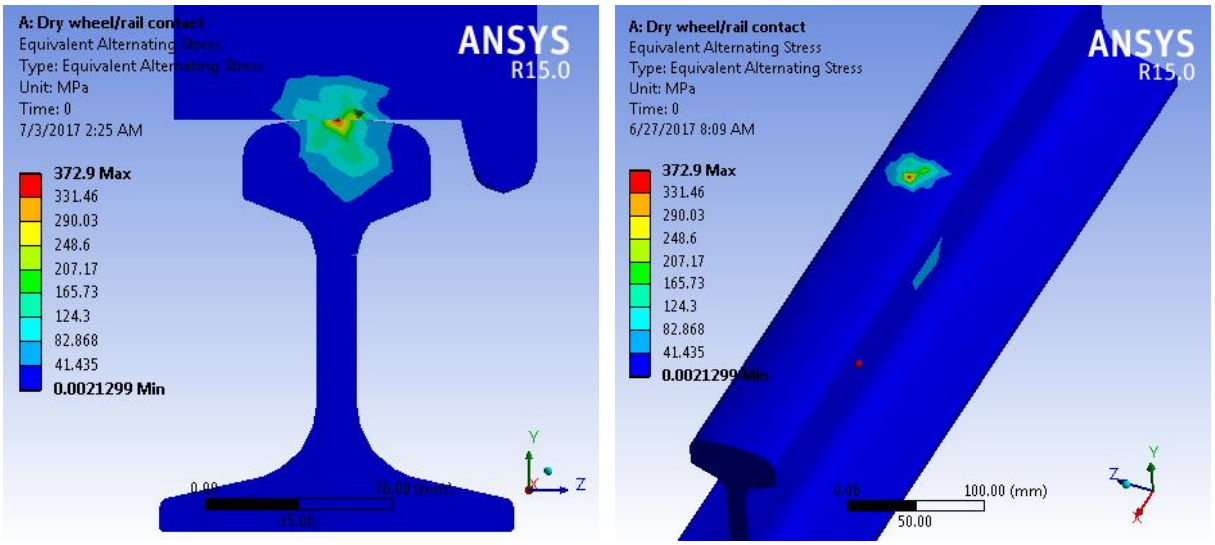

(a)

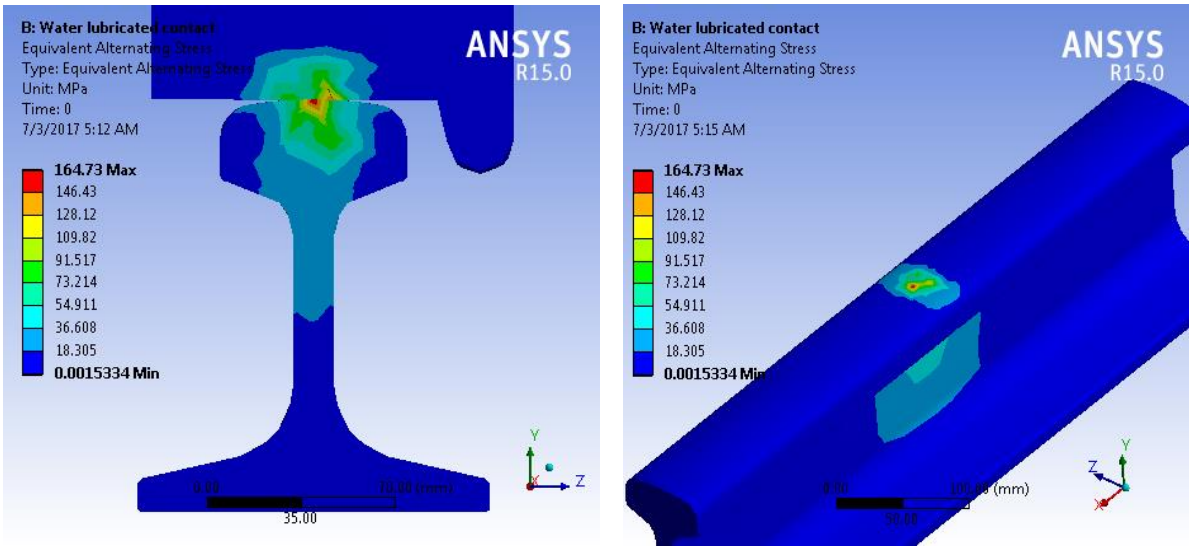

(b)

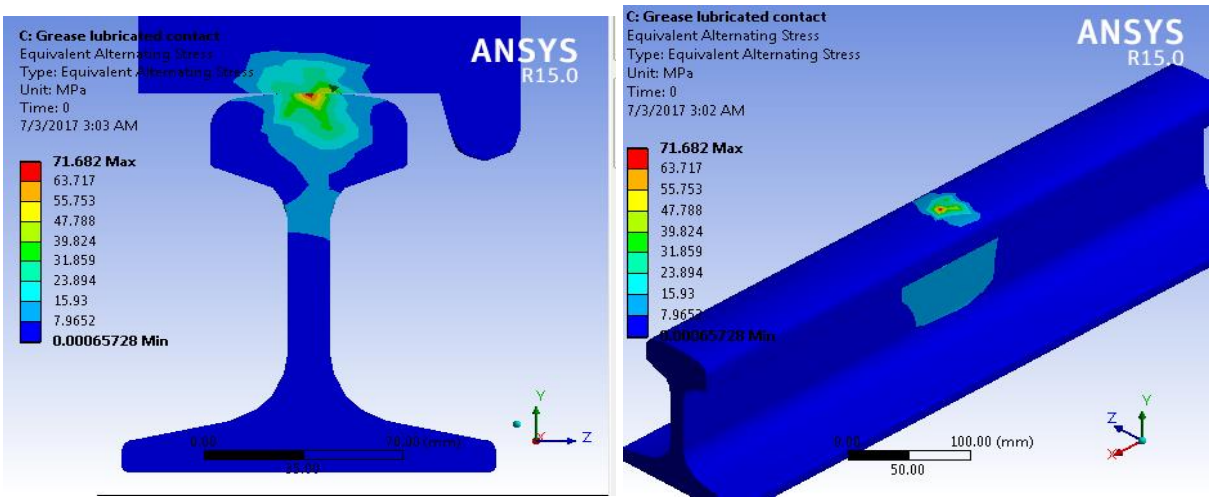

(c)

Figure 4.1-7: Equivalent alternating stress of rail under (a) dry contact (b) water lubricated contact and (c) grease lubricated contact conditions

4.1.3.4. Fatigue Safety Factor

Fatigue safety factor is a contour plot of the factor of safety with respect to a fatigue failure at a given design life. The maximum factor of safety displayed is 15. Like damage and life, this result may be scoped. For Fatigue safety factor, values less than one indicate failure before the design life has reached.

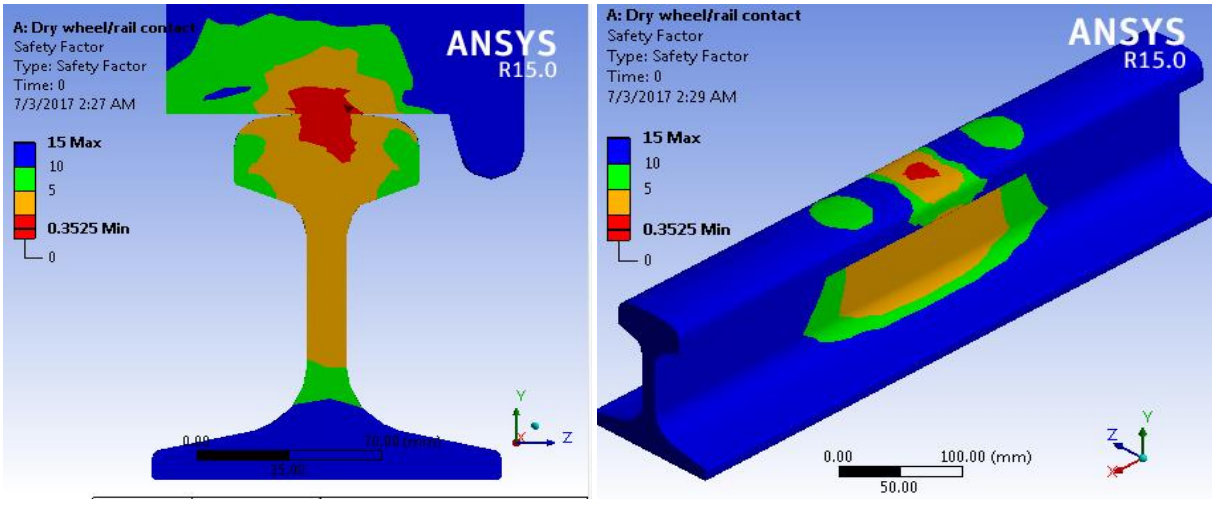

(a)

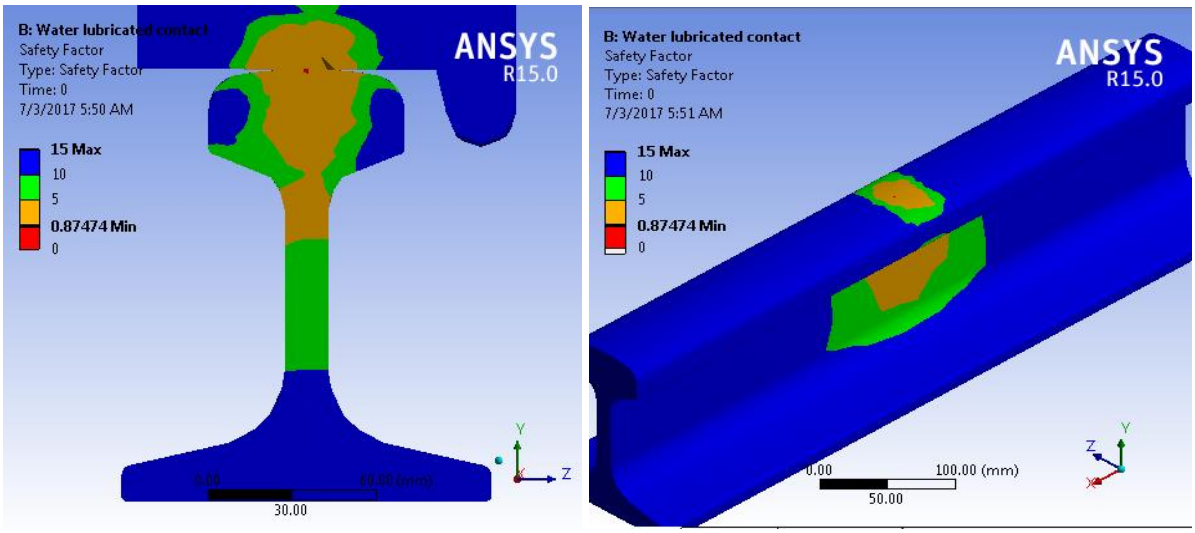

(b)

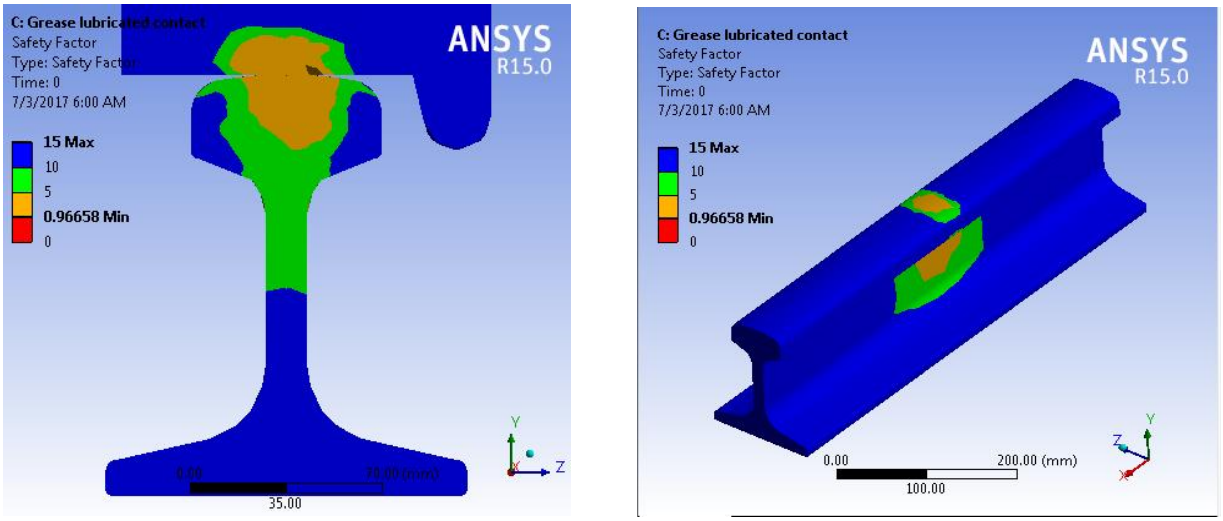

(c)

Figure 4.1-8: Fatigue safety factor of rail under (a) dry contact (b) water lubricated contact and (c) grease lubricated contact conditions

As seen from the result the fatigue safety factor is minimum under the Dry wheel/rail contact condition. This means that the rail life is safer under lubricated contact conditions since the safety factor is higher compared to the dry contact conditions.

4.2. DISCUSSION

From the above results under the same wheel/rail geometry, material property, mesh control (type & size) applied load and boundary conditions. The following results are obtained only by varying the COF. The results are summarized in the following table

	Case 1 (a) Dry contact (μ=0.6)	Case 2 (b) Water lubricated (μ=0.2)	Case 3 (c) Grease lubricated (μ=0.07)
Maximum contact pressure (MPa)	689.56	680.48	678.2
Equivalent Von misses stress (MPa)	411.89	242.59	143.36
Maximum shear stress (MPa)	215.63	132.71	74.08
Minimum Fatigue life (cycle)	3689.4	37834	1.08e5
Damage	1.356e5	26432	9259.4
Fatigue safety factor	0.35	0.87	0.967
Equivalent Alternating stress (MPa)	372.9	164.73	71.68

Table 4.2-1: Results Summery for numerical analysis

As it can be seen from the table the maximum contact pressure is almost the same under the three conditions. From this it can be see that the friction coefficient has a negligible effect on the maximum contact pressure.

The values of von-misses and maximum shear stress are significantly varied under the three wheel/rail contact condition cases. This variation is due to the varying COF under the three cases. From this it can be seen that the friction coefficient have a significant effect on the contact stresses. Under dry contact condition, where there is high COF high von-misses as well as high

maximum shear stress is generated. When there is high stress it leads to early failure to fatigue and the susceptibility to damage of the rail increase.

The results output found from this study can be validated with [3]. In the literature, varying COF's are used and the traction force, maximum contact pressure, and shear stress are calculated. The FEM output results as mentioned in table 2.3-1 show that when the friction coefficient increases the traction force and shear stress whereas the contact pressure is almost similar for all cases. This result is somewhat the same with the outputs from these results.

4.2.1. Stress -Life cycle (S-N) curve

The cyclic variation of mean stress produced by cyclic loading conditions affects the life a structure.

The SN curve is done using the equivalent stress using the Goodman's theory.

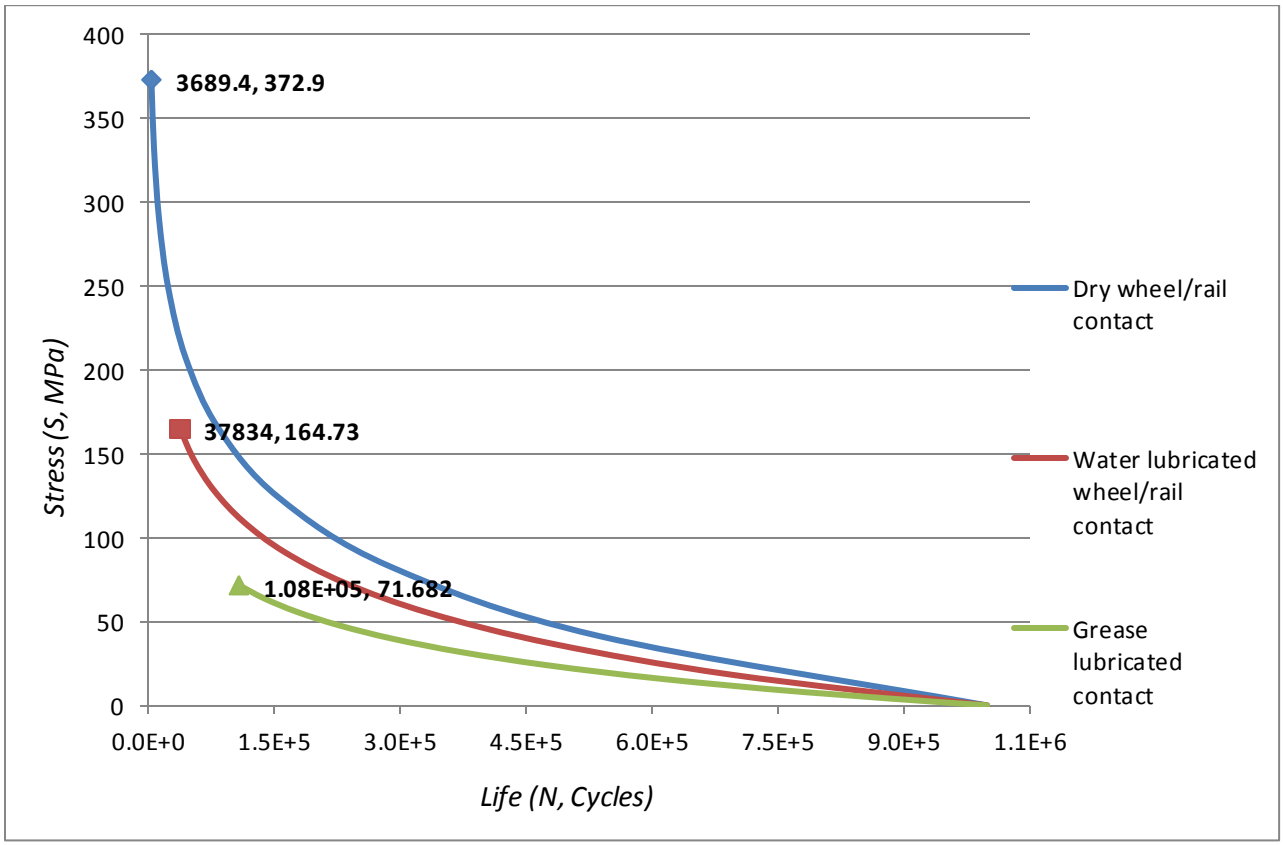

Figure 4.2-1: Relation between stress and life of the rail.

From the graph it is seen that at the point of contact where maximum equivalent alternating stress occurs the life cycle reduces. When life cycle is minimum then the stresses are maximum. So the life cycle of the rail is dependent on the stresses.

Under dry contact condition (*3689.4, 372.9)* the life cycle of the rail is minimum and the stress is high (372.9 MPa) compared to the water and grease lubricated contact condition. Since it has minimum life cycle of *3689.4 cycles* if it goes beyond that cycle value then the rail will fail.

Under water lubricated contact (37834, 164.73) the life cycle is higher than the dry contact. So the rail has more life than the dry contact condition. The same goes for grease lubricated contact. Under the grease lubricated contact the life cycle of the rail is even higher (*1.08e5*).

4.2.2. Damage –Life Cycle curve

The following graph shows the damage of the rail with regards to life cycle.

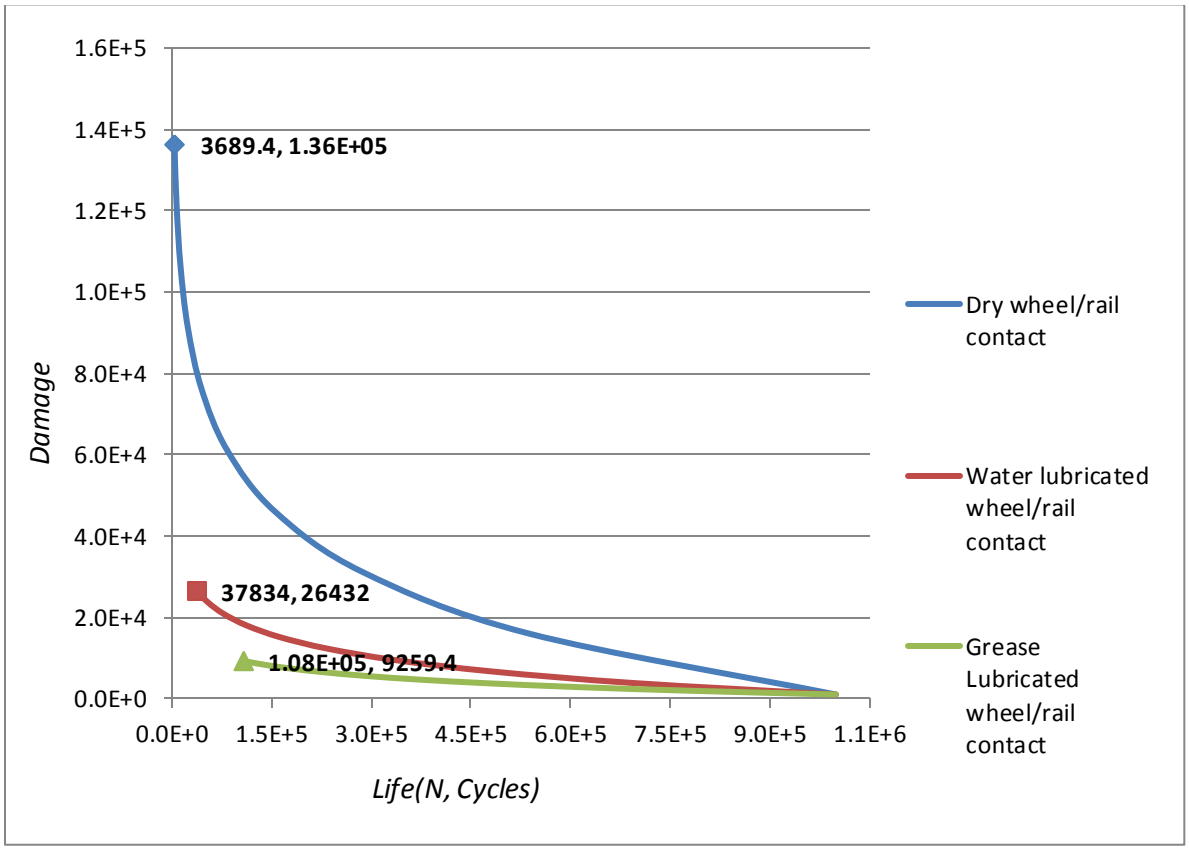

Figure 4.2-2: Relation between damage and life of the rail

From the graph it is seen that the damage increases with decreasing fatigue life, they have indirect relationship. So this means that the damage and stress have direct relations. When the stress value increases the susceptibility to damage also increases.

Under dry contact condition (*3689.4, 1.36e5*) as discussed before the life cycle of the rail is minimum, and the damage is higher (1.36e5) .Under water and grease lubricated contact conditions the damage decreases accordingly. So the fatigue damage of the rail is higher under dry contact condition.

CHAPTER FIVE: CONSCLUSION, RECOMMENDATION AND FUTURE WORK

5.1. Conclusion

This main aim of this study is to analyze the fatigue wear analysis and life prediction of rail under different wheel/rail contact conditions (dry, water lubricated, grease lubricated) due to third body materials (contaminants) present on the rail. It is known that the rail is subjected to high contact stresses of alternating magnitude due to rolling action of the wheel. Due to this the rail is prone to fatigue damage. So in this paper main emphasis is given to the wheel/rail contact since it is a critical part of safety for railway system and easily susceptible to damage. In this study the wheel/rail contact is modeled under dry, water and grease lubricated contact conditions on a straight track, considering only the wheel tread-rail head contact. The model is based on the current AA-LRT wheel/rail profiles & geometry, optimum design loads and operating system. The models are analyzed under varying coefficient of friction, 0.6 for dry, 0.2 for water lubricated, 0.05 for grease lubricated contact conditions. The study determined the contact stress states and fatigue life of the rail. From the results found it can be concluded that the friction coefficient present on the rail plays an important role in the wheel/rail traction force, contact stresses and the fatigue failure of the rail. Under dry contact where there is high COF, high traction force, high von-misses and shear stress occurs which further result in the decrease of the life of the rail. Based on the figures 4.2-1 and 4.2-2 the fatigue life of the rail is reduced (decreased) under dry condition and the damage formation is higher compared to lubricated contact conditions.

It is seen that the traction force is higher under the dry contact condition compared to water lubricated and grease lubricated contact conditions. Under the grease contact condition the traction force is very small. This can be validated with the literature [19], which says that grease contact can lead to low traction problems and poor adhesion.

.

5.2. Recommendation

This study is made based on the current AA-LRT operating system. As we know the environmental conditions vary significantly in Addis Ababa, and also contaminants (third body materials) present on the rail leads to highly variation in the friction coefficient. To maximize, (optimize) the life of the rail preventive measures should be taken. So based on the literatures reviewed and results found in this thesis the following recommendations are given:-

- Proper lubrication system must be employed since it plays an important role in increasing the life of the rail. Proper lubrication refers to the right type of lubricants and right amount of lubricants (not in excess or limited).
- The most recommended strategy is Friction management strategy to AA-LRT to operate safely. Friction management is the process of controlling the friction levels on the rail to values appropriate for operating condition. In case the friction is too high lubricants can be applied and incase the friction is too low, friction modifiers can be applied.
- Friction management strategy in the wheel/rail interface must include the straight track (top-of rail).

5.3. Future Work

The following are suggested for future work as extensions and elaborations of this research

- The present study is only made for straight track, in the future fatigue wear analysis on curved track under dry and lubricated wheel/rail contact conditions is suggested, since most damage occurs in this area.
- The friction coefficients are simply chosen in this study, for future the actual friction coefficient can be measured on the AA-LRT rail track under different environmental conditions, and further analysis can be made based the real COF data.
- The dynamic effect as well as the effects caused at braking condition can also be included in future studies.

REFERENCE

[1] DR. Richard Pankhurst, The Franco-Ethiopian Railway and its History, https://tezetaethiopia.wordpress.com , 2005.

[2] ERC. The National Railway Network of Ethiopia, http://www.erc.gov.et, 2011.

[3] K.D.Vo, A.K.Tieu, H. T. Zhu, and P. B. Kosasih, "A tool to estimate the wheel/rail contact and temperature rising under dry, wet and oily conditions," Computers in Railways XIV: Railway Engineering Design and Optimization, 2014.

[4] U. Olofsson and Roger Lewis, 'Tribology Of the wheel-Rail contact', Handbook of Railway Dynamics, Chapter Five, 2006.

[5] R. Lewis, R.S. Dwyer-Joyce, S.R. Lewis, "Tribology of the wheel-rail contact: The effect of third body materials", International Journal of Railway Technology, 2012.

[6] Yi Zhu, Adhesion in the wheel-rail contact under contaminated conditions, Royal Institute of Technology, 2011.

[7] Yi Zhu, U.Olofsson, A. Sderberg, "Adhesion modeling in the wheel-rail contact under dry and lubricated conditions using measured 3D surfaces", Tribology International, 2013.

[8] D. Raman, G. Chattodpadhyay, M. Spirigian & M. Sajjad, "Research Methodology for Evaluation of Top of Rail Friction Management in Australian Heavy Haul Networks", CRC for rail innovation, 2013.

[9] Eric E. Magel, Rolling Contact Fatigue: A comprehensive review, Center for Surface Technology, 2011.

[10] G.W Stachowiak, A.W. Batchelor , Tribology Series, ENGINEERING TRIBOLOGY ,Chapter Fourteen, Fatigue wear, 1993.

[11] Chapter Four-Introduction to wear and wear mechanisms, AAiT, PPT., 2015.

[12] N. Bosso et al., "Mechatronic Modeling of Real-time wheel rail contact-Review of wheel-rail contact Models", Springer-Verlag Berlin Heidelberg, 2013.

[13] W.Yan and F.D. Fisher, "Applicability of Hertz contact theory to rail-wheel contact problems", Archive of Applied Mechanics, 2000.

[14] Carter- F.W Carter, on the action of a locomotive driving wheel, in: proceedings of royal Society of London. Series a Vol.112, August 1926.

[15] K.L. Johonson, Contact mechanics. New York: Cambridge University press, 1985.

[16] J.J Kalker, Three-Dimensional Elastic Bodies in Rolling Contact: Springer, 1990.

[17] J.J Kalker, "wheel-rail rolling contact theory", wear, 1991.

[18] O. Polach, "A fast wheel–rail forces calculation computer code, Vehicle System Dynamics", 1999.

[19] Mesfin G/Tsadik, "Extent of adhesion losses in the wheel-rail contact under contaminated conditions" , 2014

[20] Saurabk Kumar, "Study of Rail Breaks Associated risks and Maintenance Strategies", 2006:7

[21] T. Telliskivi, U. Olofsson, "Contact mechanics analysis of measured wheel-rail profiles using the finite element method, in: Proceedings of the Institution of Mechanical Engineers", Part F: Journal of Rail and Rapid Transit, 2001.

[22] K.D. VO, A.K Tieu, H.T .Zhu, "A 3D dynamic model to investigate wheel-rail contact under High and Low adhesion", 2013.

[23] P Hosseni Tehrani, M Saket. "Fatigue crack initiation life prediction of railroad", 7th International conference on Modern practice in Stress and vibration Analysis, 2009.

[24] Olofsson and R. Nilsson "Surface Cracks and Wear of Rail: a Full-Scale Test on a Commuter Train Track", Proceedings of Institute of Mechanical Engineers, Part F: Journal of Rail and Rapid Transit, 2002.

[24] Yalcm Ozdemir, "Analysis of Normal and Tangential Wheel-Rail Contact problem with Nonlinear Material Behavior", 2016.

[25] China Railway Group (CRECG) Project Manager Office, Technical specification of vehicles, Light Rail ERC Project of Addis Ababa, Ethiopia

[26] Katrin Madler and Manfred Mannasch, material used for wheels on rolling stock, Germany, EN13262.

[27] Wakuma Guta "General Knowledge about Rolling Stock" ppt.

[28] Raymond Browell, Calculating and Displaying Fatigue Results, 2006.

[29] Contact mechanics, Chapter 3, "The contact mechanics of solids bodies such as wheel on rail",

[30] National Standards of the people's Republic of China, Hot Rolled steel rail for railway, general administration of Quality supervision, Inspection and Quarantine of the People's Republic of China ,GB2585-07-12,2007

[31] Mundisa Widhan, Pathiranage Isuru, Udara Wickramasinghe, " Investigation of Surface Ratcheting due to rail/wheel contact ", 2013.

[32] Yalcin Ozdemir "Analysis of Normal and Tangential Wheel-rail contact problem with non-linear material behavior." 2016.

[33] Babette Dirks, "Simulation and measurement of wheel on rail fatigue and wear," KTH Royal Institute of Technology, 2015

[34] KD. VO, "Damage analysis of wheel/rail contact associated to high adhesion condition", 2015

APPENDIX

Kalker's Coefficient table

	g	C_{11}			C_{22}			C_{23}		
		$\sigma=0$	$\sigma=\frac{1}{4}$	$\sigma=\frac{1}{2}$	$\sigma=0$	$\sigma=\frac{1}{4}$	$\sigma=\frac{1}{2}$	$\sigma=0$	$\sigma=\frac{1}{4}$	$\sigma=\frac{1}{2}$
	$\downarrow 0$	$\left[\frac{\pi^2}{4(1-\sigma)}\right]$			$\left[\frac{\pi^2}{4}\right]$			$\left[\frac{\pi g^{1/2}}{3(1-\sigma)}\{1+\sigma(\frac{1}{4}\Lambda+\ln 4-5)\}\right]$		
$b>a$	0.1	2.51	3.31	4.85	2.51	2.52	2.53	0.334	0.473	0.731
	0.2	2.59	3.37	4.81	2.59	2.63	2.66	0.483	0.603	0.809
	0.3	2.68	3.44	4.80	2.68	2.75	2.81	0.607	0.715	0.889
	0.4	2.78	3.53	4.82	2.78	2.88	2.98	0.720	0.823	0.977
	0.5	2.88	3.62	4.83	2.88	3.01	3.14	0.827	0.929	1.07
	0.6	2.98	3.72	4.91	2.98	3.14	3.31	0.930	1.03	1.18
	0.7	3.09	3.81	4.97	3.09	3.28	3.48	1.03	1.14	1.29
	0.8	3.19	3.91	5.05	3.19	3.41	3.65	1.13	1.25	1.40
	0.9	3.29	4.01	5.12	3.29	3.54	3.82	1.23	1.36	1.51
	1.0	3.40	4.12	5.20	3.40	3.67	3.98	1.33	1.47	1.63
$a>b$	0.9	3.51	4.22	5.30	3.51	3.81	4.16	1.44	1.59	1.77
	0.8	3.65	4.36	5.42	3.65	3.99	4.39	1.58	1.75	1.94
	0.7	3.82	4.54	5.58	3.82	4.21	4.67	1.76	1.95	2.18
	0.6	4.06	4.78	5.80	4.06	4.50	5.04	2.01	2.23	2.50
	0.5	4.37	5.10	6.11	4.37	4.90	5.56	2.35	2.62	2.96
	0.4	4.84	5.57	6.57	4.84	5.48	6.31	2.88	3.24	3.70
	0.3	5.57	6.34	7.34	5.57	6.40	7.51	3.79	4.32	5.01
	0.2	6.96	7.78	8.82	6.96	8.14	9.79	5.72	6.63	7.89
	0.1	10.7	11.7	12.9	10.7	12.8	16.0	12.2	14.6	18.0
	$\downarrow 0$	$\left[\frac{2\pi}{(\Lambda-2\sigma)g}\left(1+\frac{3-\ln 4}{\Lambda-2\sigma}\right)\right]$			$\left[\frac{2\pi}{\{(1-\sigma)\Lambda+2\sigma\}g}\left(1+\frac{(1-\sigma)(3-\ln 4)}{(1-\sigma)\Lambda+2\sigma}\right)\right]$			$\left[\frac{2\pi}{3g^{3/2}}\frac{1}{(1-\sigma)\Lambda-2+4\sigma}\right]$		